

# Snow Water Equivalents exclusively from Snow Depths and their temporal Changes: The $\Delta$ SNOW.MODEL

Michael Winkler<sup>1,\*</sup>, Harald Schellander<sup>1,2,\*</sup>, and Stefanie Gruber<sup>1</sup>

<sup>1</sup>ZAMG – Zentralanstalt für Meteorologie und Geodynamik, Innsbruck, Austria

<sup>2</sup>Department of Atmospheric and Cryospheric Sciences, University of Innsbruck, Austria

\*These authors contributed equally to this work.

**Correspondence:** Michael Winkler (michael.winkler@zamg.ac.at) and Harald Schellander (harald.schellander@zamg.ac.at)

**Abstract.** Snow depths have been manually observed for many years, sometimes decades, at various places around the globe. These records are often of good quality. In addition, more and more data from automatic stations and remote sensing are available. On the other hand, records of snow water equivalent (*SWE*) – synonymous for snow load or mass – are sparse, although it might be the most important snowpack feature in hydrology, climatology, agriculture, natural hazards research, etc. *SWE* very often has to be modeled, and respective models either depend on meteorological forcing or are not intended to simulate individual *SWE* values, like the substantial seasonal “peak *SWE*”.

The  $\Delta$ SNOW.MODEL is presented as a new method to simulate local-scale *SWE*. It solely needs a regular time series of snow depths as input. The  $\Delta$ SNOW.MODEL is a semi-empirical multi-layer model and freely available as R-package. Snow compaction is modeled following the rules of Newtonian viscosity. The model considers measurement errors, treats overburden loads due to new snow as additional unsteady compaction, and melted mass is stepwise distributed top-down in the snowpack.

Seven model parameters are subject to calibration. Snow observations of 67 winters from 14 stations, well-distributed over different altitudes and climatic regions of the Alps, are used to find an optimal parameter setting. Data from another 71 independent winters from 15 stations is used for validation. Results are very promising: Median bias and root mean square error for *SWE* are only  $-3.0 \text{ kg m}^{-2}$  and  $30.8 \text{ kg m}^{-2}$ , and  $+0.3 \text{ kg m}^{-2}$  and  $36.3 \text{ kg m}^{-2}$  for peak *SWE*, respectively. This is a major advance compared to snow models relying on empirical regressions and even sophisticated thermodynamic snow models do not necessarily perform better.

## 1 Introduction

Depth (*HS*) and bulk density ( $\rho_b$ ) are fundamental characteristics of a seasonal snowpack (e.g., Goodison et al., 1981; Fierz et al., 2009). Equation (1) links them to the areal density [ $\text{kg m}^{-2}$ ] of the snowpack, which – in hydrological applications – is

20 usually referred to as snow water equivalent ( $SWE$ ), as it resembles “the depth of water that would result if the mass of snow melted completely” (Fierz et al., 2009).

$$SWE = HS \cdot \rho_b \tag{1}$$

[1 kg m<sup>-2</sup>  $\equiv$  1 mm water equivalent (w.e.)]

### 1.1 Measurements of $HS$ and $SWE$

Measuring  $HS$  is relatively easy (e.g., Sturm and Holmgren, 1998): Manual measurements at a certain point only require a rod  
25 or ruler (e.g., Kinar and Pomeroy, 2015), and decades-long series of daily  $HS$  measurements exist in many regions – in lowlands as well as in alpine areas (e.g., Haberkorn, 2019). In modern times more and more  $HS$  data from automated measurements (mostly sonic or laser distance ranging) become available, typically in sub-hourly resolution (McCreight and Small, 2014). In addition, remote sensing techniques currently increase the number of  $HS$  data significantly, having the advantage of an areal picture instead of point information but at the cost of accuracy and in most cases also temporal resolution and regularity (Cf.,  
30 e.g., Dietz et al. (2012) for a general review of methods, and Deems et al. (2013) for a review on lidar measurements. Painter et al. (2016) provide a thorough overview. Garvelmann et al. (2013) and Parajka et al. (2012), e.g., illustrate the potential of timelapse photography.)

In contrast, measurements of  $SWE$  (or  $\rho_b$ ) are more difficult (e.g., Sturm et al., 2010): Manual measurements require some basic equipment like snow tubes or snow sampling cylinders, a bit of dexterity, and are time consuming. In case snow  
35 depth exceeds the sampling tool’s size a pit has to be dug to consider the layered structure of the snowpack (e.g., Kinar and Pomeroy, 2015). As a consequence,  $SWE$  measurements are carried out at much fewer locations than  $HS$  measurements (e.g., Mizukami and Perica, 2008; Sturm et al., 2010), their accuracy is lower, and series are shorter. Only in very rare cases consecutive, decades-long measurement series are available (e.g., in Switzerland; cf. Jonas et al., 2009). Often they are only carried out at irregular time intervals (“snow courses”) and even if regularly measured, temporal resolution is hardly ever higher  
40 than two weeks. Also automatic measurements of  $SWE$  are not at all comparable in quality and quantity with automated  $HS$  measurements. They are quite expensive, often inaccurate, still at a developmental stage, and/or suffer from significant problems if not intensively maintained throughout the snowy season. Methods involve weighing techniques (snow scales; e.g., Smith et al., 2017; Johnson et al., 2015), pressure measurements (snow pillows; e.g., Goodison et al., 1981), upward-looking ground penetrating radar (e.g., Heilig et al., 2009), passive gamma radiation (e.g., Smith et al., 2017), cosmic ray neutron  
45 sensing (e.g., Schattan et al., 2019), L-band Global Navigation Satellite Signals (e.g., Koch et al., 2019), etc. Presumably, the biggest and best serviced network of automated  $SWE$  measurements is SNOTEL with about 800 sites in Western North America (Avanzi et al., 2015).

$SWE$  data from remote sensing are not operationally available for the local and point scale, and deriving this snow property from satellite products at sub-kilometer resolution is still not possible (Smyth et al., 2019). On top of that, there is the issue  
50 of longterm availability: automated measurements and at least rough remote sensing of  $SWE$  have not been available for

more than some twenty years at their best (e.g., SNOTEL, operated since the late 1990s), a fairly short timespan compared to decades-long daily  $HS$  data (e.g., Kinar and Pomeroy, 2015).

Regardless of these problematic circumstances accompanying  $SWE$  measurements, many hydrological, agricultural, and other applications depend on good estimates of  $SWE$  (e.g., Goodison et al., 1981; Sturm and Holmgren, 1998). Ultimately, the mass of water stored in the snowpacks matters very often and, therefore, the majority of those fields is especially interested in seasonal  $SWE$  maxima, i.e. “peak  $SWE$ ” ( $SWE_{pk}$ ).  $SWE_{pk}$  are also the main focus of different kinds of extreme value and climatic analyses, both of which additionally very much rely on longterm or even “historical” data. Not least, snow load standards (e.g., International Organization for Standardization, 2013) rely on extreme value analyses of longterm  $SWE$  records, as snow load is defined as the product of  $SWE$  and the gravitational acceleration. These points reveal the great discrepancy between the good data situation in terms of  $HS$  on the one hand, and the insufficient availability of  $SWE$  data on the other.

## 1.2 Modeling $SWE$

Modern snow models like Crocus (e.g., Vionnet et al., 2012), SNOWPACK (e.g., Lehning et al., 2002), SNTHERM (Jordan, 1991), or the dual-layer model SNOBAL (Marks et al., 1998) resolve mass and energy exchanges within the ground-snow-atmosphere regime in a detailed way by depicting the layered structure of seasonal snowpacks. Echoing Langlois et al. (2009), these models will be termed “thermodynamic snow models” in the following. All of them need atmospheric variables as input, primarily precipitation, temperature, humidity, wind speed, and radiative fluxes. Also relatively simple thermodynamic models at least require temperature and/or precipitation (e.g., De Michele et al., 2013) or climatological means thereof (Hill et al., 2019). Avanzi et al. (2015) provide a good review. Unfortunately, many valuable longterm  $HS$  series do not involve these data, and parameterizing or downscaling them from other sources in turn is susceptible to errors. Thermodynamic snow models are not applicable to derive  $SWE$  exclusively from  $HS$ .

On the other side of the  $SWE$  modeling spectrum there are those models which – aside  $HS$  – only depend on date  $d$  (Pistocchi, 2016),  $d$  and altitude  $z$  (Gruber, 2014, see statistical approach therein),  $d$  and regional parameters (e.g., Mizukami and Perica, 2008; Guyennon et al., 2019) or  $d$ ,  $z$  and regional parameters (e.g., Jonas et al., 2009). Again, Avanzi et al. (2015) provide a thorough listing of those models, which will be termed “empirical regression models” (ERMs) in the following. ERMs very much rely on the strong, near-linear dependence between  $HS$  and  $SWE$  (cf., e.g., Jonas et al., 2009). According to Gruber (2014) and Valt et al. (2018)  $HS$  describes 81% and 85% of  $SWE$  variance, respectively. This behavior bases on the narrow range within which the majority of bulk snow densities is found, and it leads to the well-known characteristic of  $HS$ – $SWE$ – $\rho_b$  datasets: log-normally distributed  $HS$  and  $SWE$  as well as normally distributed  $\rho_b$  (e.g., Sturm et al., 2010). Unfortunately, ERMs cannot adequately model (unchanged)  $SWE$  during periods with snow densification only due to metamorphism and deformation (Jordan et al., 2010) but without mass loss.

Interestingly, in most ERMs absolute, single-day  $HS$  observations are the only snow characteristics used. Depending on calibration focus they either adequately model mean- $SWE$  or  $SWE_{pk}$ , mid winter or spring, etc. This is an inherent fact due to their model architecture. Those calibrated for good estimates of mean- $SWE$  fail to model  $SWE_{pk}$  sufficiently well, those designed for  $SWE_{pk}$  often give bad  $SWE$  results during phases with shallow snowpacks. Typically, they simulate unrealistic

85 mass losses during phases with compaction only by metamorphism and deformation, and the timing of  $SWE_{pk}$  as well as the duration of high snow loads cannot be modeled well. As it is honestly stated by Jonas et al. (2009) those models cannot be used to “convert time series of  $HS$  into  $SWE$  at daily resolution or higher” because they may “feature an incorrect fine structure in the temporal course of  $SWE$ ”. Therefore, ERMs are not suitable to calculate  $SWE$  for individual days.

90 McCreight and Small (2014) go an interesting step further and not only use single-day  $HS$  values for their regression model, but also the “evolution” of daily  $HS$ . They make use of the negative correlation of  $HS$  and  $\rho_b$  at short timescales (10 days) and their positive/negative correlation at longer timescales (3 months) during accumulation/ablation phases. This promising step of development is limited by the fact that the model parameters can only be estimated through regressions relying on at least three training datasets of  $HS$  and  $\rho_b$  from nearby stations. Unfortunately, this disqualifies the model of McCreight and Small (2014) for assigning  $SWE$  to longterm and historical  $HS$  series as consecutive  $SWE$  measurements are not available for those.

95 An alternative approach that links  $HS$  and  $SWE$  throughout a snowy season without the need of further meteorological input is provided by Martinec (1977) and revisited by Martinec and Rango (1991). In some respect their semi-empirical model bridges the gap between thermodynamic models and ERMs. They use a method already developed by Martinec (1956) “to compute the water equivalent from daily total depths of the seasonal snow cover”. Snow compaction is expressed as a time-dependent power function. Each layer’s snow density  $\rho_n$  after  $n$  days is given by  $\rho_n = \rho_0 \cdot (n + 1)^{0.3}$ , where  $\rho_0$  is the initial density of the snow layer. A fixed exponent of 0.3 is used, without going into detail. Martinec and Rango (1991) set  $\rho_0$  to 100 kg m<sup>-3</sup>, Martinec (1977) varied it from 80 to 120 kg m<sup>-3</sup>. This computation is meant to give good results for the seasonal maximum snow water equivalent ( $SWE_{pk}$ ). It is shown, the older the snow the less important is the correct choice of the crucial parameter  $\rho_0$  (Martinec, 1977; Martinec and Rango, 1991). Their model interprets “each increase of total snow depth [...] as snow fall” and if “the total snow depth remains higher than the settling by [the power function], this is also interpreted as new snow. If the snow depth drops lower than the value of the superimposed settling curve of the respective snow layers, it is interpreted as snowmelt, and a corresponding water equivalent is subtracted. In this way the water equivalent of the snow cover can be continuously simulated [...]” (Martinec and Rango, 1991). Rohrer and Braun (1994) improved this model particularly for the ablation season by further increasing density whenever melt conditions are modelled and by introducing a maximum possible snow density of 450 kg m<sup>-3</sup>.

110 Table 1 summarizes the classification of  $SWE$  models with respect to their essential input.

### 1.3 Motivation for a New Approach

The question evolves, whether those semi-empirical, layer-resolving snow models can be improved and modernized, in order to provide an up-to-date snow model standard between sophisticated, thermodynamic models and modest ERMs. Looking at the ease of Martinec (1977)’s and Rohrer and Braun (1994)’s approaches requiring only regular  $HS$  as input (see Table 1), 115 thinking about modern computational possibilities, and given the introductorily described strong need for an implementable method, it seems interesting that there are no recent publications on this topic.

In the following, an advancement of semi-empirical *SWE* models is presented, which maintains their key feature of considering daily *change* of snow depth as a proxy for the various processes altering bulk snow density and snow water equivalent, but further

- 120 – bases its (dry) snow densification function on Newtonian viscosity,
- provides a way to deal with small discrepancies between model and observation (in the order of *HS* measurement errors),
- takes into account unsteady compaction of underlying, older snow layers due to overburden snow loads, and
- densifies snow layers from top to bottom during melting phases without automatically modeling mass loss due to runoff.

The ideas for the latter three features were already developed by Gruber (2014), but not suitably realized. The new modeling  
125 approach is named  $\Delta$ SNOW.MODEL and an easy-to-use R-package is available through <https://cran.r-project.org/package=nixmass>. The package is called *nixmass*, and it not only involves the  $\Delta$ SNOW.MODEL, but also other models that use snow depth (*nix*... Latin for “snow”) to simulate *SWE* (i.e., snow *mass*).

The way how physical processes are coded in the  $\Delta$ SNOW.MODEL is thoroughly described in the Method section of this publication (Sect. 2). The calibration is outlined in Sect. 2 as well. Results, like best parameter choices and validation of the  
130 model output, are given in Sect. 3. In Sect. 4 model sensitivity, open questions, and possible future developments are discussed and Sect. 5 provides concluding remarks.

## 2 Method

Snow compacts over time due to various processes. Jordan et al. (2010) categorize them in snow drift, dry and wet metamorphism, and deformation. The  $\Delta$ SNOW.MODEL cannot deal with snow drift, however, it differentiates between the latter  
135 processes: Dry metamorphism is mainly processed in the *Dry Compaction module* of the  $\Delta$ SNOW.MODEL, in case of a significant increase in snow depth also in the *Overburden submodule* of the *New Snow module*. Wet metamorphism is treated in the *Drenching module*. The fourth module of the  $\Delta$ SNOW.MODEL, the *Scaling module*, accounts for small discrepancies between model and observations. Table 2 correlates Jordan et al. (2010)’s compaction processes with the  $\Delta$ SNOW.MODEL modules and outlines the processes that are ignored. The specific modules are described in Sects. 2.1 and 2.2, a scheme of the model  
140 principle is shown in Fig. 1.

### 2.0.1 Preliminary: The First Snow Layer

For non-zero snow depth observations ( $HS_{\text{obs}} > 0$ ) after a snow-free period the  $\Delta$ SNOW.MODEL assigns the following features to the model snowpack: There is one snow layer (layer counter  $ly = 1$ ) and the age of this layer is set to  $age = 1$ . Thickness of this model layer ( $hs$ ) and total model snow depth ( $HS$ ) are equal, and set to observed snow depth:  $hs = HS := HS_{\text{obs}}$ .  
145 Analogously, the layer’s snow water equivalent equals total snow water equivalent:  $swe = SWE := \rho_0 \cdot HS_{\text{obs}}$ , with new snow

density  $\rho_0$  being an important parameter of the  $\Delta$ SNOW.MODEL (cf. Sect. 3). The treatment of the first snow event is illustrated at  $t = 2$  in Fig. 1.

## 2.1 Dry Compaction module

As it was mentioned in the Introduction, Martinec and Rango (1991) used a power function to describe densification of aging snow, because this way errors in initial density  $\rho_0$  get less relevant over time. For the  $\Delta$ SNOW.MODEL this kind of high error tolerance of  $\rho_0$  is a rather feeble argument to use a power law, since it only holds for old snow and deep snowpacks, but with the  $\Delta$ SNOW.MODEL also  $SWE$  of ephemeral snowpacks (e.g., at low elevation sites) should be modeled as good as possible. Furthermore, as the  $\Delta$ SNOW.MODEL considers overburden load in a particular way (Sect. 2.2.1), it is not expedient to have a direct dependence between density and age of a layer. Aside from that drawbacks of a power law compaction and in contrast to Martinec and Rango (1991)'s unproven claim “snow would [not] settle [...] according to an exponential curve”, most modern snow models simulate snow compaction by way of Newtonian viscosity with associated exponential densification over time (e.g., Jordan et al., 2010). In the  $\Delta$ SNOW.MODEL's *Dry Compaction module* the densifying effects of dry metamorphism and deformation are combined, by applying the following adaption of Sturm and Holmgren (1998)'s relation, with the help of De Michele et al. (2013).

$$\frac{hs(i, t-1)}{hs(i, t)} = 1 + \Delta t \cdot \frac{\hat{\sigma}(i, t)}{\eta(i, t)}$$

$$\text{with } \hat{\sigma}(i, t) = g \cdot \sum_{\hat{i}=i}^{ly(t)} swe(\hat{i}, t) \quad (2)$$

$$\text{and } \eta(i, t) = \eta_0 \cdot e^{k \cdot \rho(i, t)}$$

Model timestep  $\Delta t$  in general is arbitrary, but usually it is one day. If so,  $t$  can be explained as “today” and  $t-1$  as “yesterday” here. Accordingly,  $hs(i, t)$  is today's modeled thickness of the  $i$ -th snow layer. Snow layers are counted from bottom to top; layer  $i = 1$  is the lowest and oldest layer. Today's depth of the total snowpack is  $HS(t) = \sum_i hs(i, t)$ .

The individual snow water equivalents of the layers are given by  $swe(i, t)$ , and their sum represents total mass of the snowpack  $SWE(t) = \sum_i swe(i, t)$ . The vertical stress at the bottom of layer  $i$  is given by  $\hat{\sigma}(i, t)$  (De Michele et al., 2013). It is constituted by the sum of loads overlying layer  $i$  (including layer  $i$ 's own load), with  $ly(t)$  being today's total number of snow layers or – in other words –  $ly(t)$  is the index  $i$  of today's uppermost (i.e., “surface”) layer.

The Newtonian viscosity of snow  $\eta$  is made density-dependent in the framework of the  $\Delta$ SNOW.MODEL (following Kojima, 1967), but dependencies on temperature, grain characteristics etc. are very consciously ignored – due to the lack of information on it when dealing with pure snow depth data. Today's density of layer  $i$  is  $\rho(i, t)$ ; it equals  $\frac{swe(i, t)}{hs(i, t)}$ .  $k$  and  $\eta_0$  are tuning parameters of the *Dry Compaction module* (see Sect. 3).

To avoid excessive compaction a crucial parameter is introduced in the  $\Delta$ SNOW.MODEL, as it was already done by Rohrer and Braun (1994):  $\rho_{\max}$ . It defines the maximal possible density of a snow layer and, consequently, also the maximum bulk snow density. Rohrer and Braun (1994) set  $\rho_{\max}$  to  $450 \text{ kg m}^{-3}$ ; finding its optimal value for the  $\Delta$ SNOW.MODEL is subject to

175 calibration (Sect. 2.3).  $\rho_{\max}$  figures the density a snow layer or the whole snowpack can reach at most, unless it loses mass by melting.  $\rho_{\max}$ , of course, is a model parameter and cannot be observed in real snowpacks. In case the *Dry Compaction module* increases the density of one or more layers beyond  $\rho_{\max}$ ,  $\rho(i, t)$  of the respective layer(s) is set equal to  $\rho_{\max}$ .

According to Eq. (2) the rate of densification of a certain snow layer is linearly depending on the overlying snow load  $\hat{\sigma}(i, t)$  and exponentially depending on the layer's density  $\rho(i, t)$ . Sturm and Holmgren (1998) conclude that this difference is one  
180 reason why "snow load plays a more limited role in determining the compaction behavior than grain and bond characteristics and temperature". Denser and older layers compact less than newer layers with lower densities. This links the densification rate to the layer age, but indirectly by the use of density, and not directly as it was the case with Martinec and Rango (1991)'s power law approach.

The *Dry Compaction module* of the  $\Delta$ SNOW.MODEL is illustrated by the light blue arrows in Fig. 1. This module is applied  
185 at every point in time (except if there is no snow; see  $t = 1$  in Fig. 1). The *Dry Compaction module* is the core module because based on its result the  $\Delta$ SNOW.MODEL decides between three different processes, realized by the other three modules:

## 2.2 Process Decisions

At every point in time, after the *Dry Compaction module* was run, observed  $HS_{\text{obs}}(t)$  and modeled  $HS(t)$  are compared. The  $\Delta$ SNOW.MODEL's process decision algorithm now takes the result of the difference  $\Delta HS(t) = HS_{\text{obs}}(t) - HS(t)$  and confronts  
190 it with  $\tau$  [m].  $\tau$  is another tuning parameter of the  $\Delta$ SNOW.MODEL (see Sect. 2.3). Technically,  $\tau$  is a threshold deviation and defines a limit of  $\Delta HS(t)$  whose overshooting, adherence, and undershooting heads for one out of the modules described in the following Sects. 2.2.1 to 2.2.3. Table 2 links them to snow physics.

### 2.2.1 New Snow module

In case  $\Delta HS(t) > +\tau$ , meaning observed snow depth is significantly higher than modeled snow depth, a new snow event is  
195 supposed and a new top snow layer is modeled by the  $\Delta$ SNOW.MODEL (see at  $t = 2$  and  $t = 7$  in Fig. 1). This is a consequential step and nothing innovative at all. Other models have implemented this mechanism as well (e.g., Martinec and Rango, 1991; Lehning et al., 1999; Sturm et al., 2010). However, the  $\Delta$ SNOW.MODEL goes beyond and introduces another feature: It explicitly models the peculiar effect of overburden load on underlying layers, defined as their enhanced densification due to stress, which is put on by the weight of new snow. Grain bonds get broken, grains slide, partially melt, and warp (Jordan et al., 2010),  
200 and the layers densify comparatively rapidly and strongly. The  $\Delta$ SNOW.MODEL interprets overburden load as an "unsteady and discontinuous" stress on the snowpack, under which snow presumably does not react as a viscous Newtonian fluid. As long as the time between two consecutive observations  $\Delta t$  is in the order of at least some hours, discontinuity is an intrinsic feature of the process.

The *New Snow module* realizes the effect of overburden load through the *Overburden submodule* by reducing each layer's  
 205 thickness  $hs(i, t)$  with the help of the dimensionless “overburden strain”  $\epsilon(i, t)$ , defined as

$$\epsilon(i, t) = c_{ov} \cdot \sigma_0 \cdot e^{-k_{ov} \frac{\rho(i, t)}{\rho_{max} - \rho(i, t)}} \quad (3)$$

with  $\sigma_0 = \Delta HS(t) \cdot \rho_0 \cdot g$ .

$c_{ov}$  [ $\text{Pa}^{-1}$ ] is another tuning parameter of the model (see Sect. 2.3) and controls the importance of the unsteady compaction due to overburden load. According to Sturm and Holmgren (1998) and in consistency with Eq. (2) snow load has a linear effect on the bulk density. Therefore,  $\epsilon(i, t)$  is made linearly depending on the load, which the overlying new snow is putting on the  
 210 underlying layers. This load is well approximated by  $\sigma_0$  [ $\text{Pa}$ ]; the bigger the overburden load, the stronger the compaction. (The overburden load does not fully equal  $\sigma_0$ , since  $\Delta HS(t)$  is not the depth of the new snow, but the difference between modeled depth “before” knowing about the new snow event and observed depth “after” the new snow event. An iterative calculation would be more precise, however, Eq. (3) proved to be an adequate compromise between simplicity and accuracy.) In order to avoid  $\epsilon(i, t) > 1$ ,  $c_{ov}$  is restricted at least to the range of values between 0 and the minimum value of the data record for  $\frac{1}{\sigma_0}$ . As  
 215  $\sigma_0$  hardly ever exceeds 1000 Pa,  $\frac{1}{\sigma_0}$  normally is larger than  $1 \times 10^{-3} \text{ Pa}^{-1}$ . This value, thus, marks a good upper bound for  $c_{ov}$  (Sect. 2.3). Dimensionless  $k_{ov}$  controls the role of a certain snow layer's density on  $\epsilon(i, t)$ , and has to be specified by calibration (see Sect. 2.3). The density-dependence of  $\epsilon(i, t)$  was chosen to be exponential, and using  $\rho_{max}$  in the denominator of Eq. (3)'s exponent secures that overburden loads cannot make snow layers denser than  $\rho_{max}$ . The closer a snow layer's density is to the maximum density  $\rho_{max}$ , the less it will be compacted by additional load. Relatively new and, therefore, not very dense layers  
 220 are exposed to greater densification, which is exactly what is observed in reality. As it will be shown in sections 2.2.2 and 2.2.3  $\rho_{max}$  also governs mass loss and melt in the model. Not least,  $\rho_{max}$  illustrates the possible maximum density of a wet seasonal snowpack in the  $\Delta$ SNOW.MODEL-world and it is possible to assign a reasonable value to it (cf. Sect. 3).

The “overburden strain”  $\epsilon(i, t)$  theoretically lies between 0 and 1 and compresses all snow layers of the model in case of a new snow event. Practically,  $\epsilon(i, t)$  is often close to zero (in this study 90% of all computed  $\epsilon$  are smaller than 0.09) and  
 225 extremely rarely higher than 0.3 (in this study only 9 out of 10000).

The following intermediate (asterisked) variables are defined due to the overburden load. The compressed layer's masses,  $swe(i, t)$ , remain unaffected during this process.

$$\epsilon(i, t) = \frac{hs(i, t) - hs^*(i, t)}{hs(i, t)} \quad \text{leading to} \quad hs^*(i, t) = (1 - \epsilon(i, t)) \cdot hs(i, t)$$

$$HS^*(t) = \sum_i hs^*(i, t) \quad (4)$$

$$\rho^*(i, t) = \frac{swe(i, t)}{hs^*(i, t)}$$



A new snow event, identified by the condition  $\Delta HS(t) > +\tau$ , of course not only impacts the older snow and compacts it  
 230 more strongly, but it also adds a new snow layer and mass to the snowpack (pink arrow at  $t = 2$  and  $t = 7$  in Fig. 1). The  
 number of layers is increased by one and the following attributes are given to the new layer:

$$\begin{aligned}
 age(ly, t) &= 1 \\
 hs(ly, t) &= HS_{obs}(t) - HS^*(t) \\
 swe(ly, t) &= hs(ly, t) \cdot \rho_0
 \end{aligned}
 \tag{5}$$

The total snow water equivalent is risen:  $SWE(i, t) = SWE(i, t - 1) + swe(ly, t)$ , and the intermediate variables of Eq. (4)  
 overwrite their originals:  $hs(i, t) = hs^*(i, t)$ ,  $HS(t) = HS^*(t) + hs(ly, t)$ , and  $\rho(i, t) = \rho^*(i, t)$ . The model-snowpack with this  
 235 new properties now again compacts according to Eq. (2), time  $t$  is risen by one increment, and at the next point in time the  
 process again starts with the decision described in Sect. 2.2. The *Overburden submodule* is illustrated with a purple arrow at  
 $t = 7$  in Fig. 1.

## 2.2.2 Scaling module

Equations (2) and (3) are highly simplified representations of the complex viscoelastic behavior of snow. Still, also snow depth  
 240 observations typically only show an accuracy of a few centimeters. The  $\Delta$ SNOW.MODEL accepts these inherent inaccuracies  
 and apparent discrepancies between model and measurements and copes with them by not applying too strict criteria in the  
 process decisions described in Sect. 2.2. The threshold deviation  $\tau$  acts as a buffer to avoid too frequent gain or loss of mass in  
 the model world: In case  $|\Delta HS| \leq |\tau|$  neither the snowpack loses mass nor gains mass, but mass is kept constant. In order to  
 benefit from having a new measurement at every point in time,  $HS(t)$  is intentionally set to  $HS_{obs}(t)$  by the *Scaling module*.

245 The *Scaling module* forces a partial reevaluation of the previous compaction, which was modeled by the *Dry Compaction*  
*module* between  $t - 1$  and  $t$ . The best-fitted parameter setting for  $\eta_0$  is temporarily rejected and substituted by  $\eta_0^*$ . It would be  
 straight forward to use one adjusted  $\eta_0^*(t)$  for all layers. However, this leads to a rational function with multiple solutions for  
 $\eta_0^*(t)$ , making it necessary to calculate different  $\eta_0^*(i, t)$  for each layer  $i$ . See Appendix B for details on that.

$\eta_0^*(i, t)$  is then used instead of  $\eta_0$  in Eq. (2) to recalculate the compaction of individual layers.  $HS(t)$  now equals  $HS_{obs}(t)$ .  
 250 In most cases all layers get “slightly more” or “slightly less” compacted by the *Scaling module* than by the *Dry Compaction*  
*module*. Only at rare occasions the scaling does not compact, but a small “stretching” of the snowpack is necessary. This  
 only happens if there was a small increase in observed snow depth *and* very little modeled dry metamorphic compaction; the  
 condition  $HS(t) + \tau > HS_{obs}(t) > HS_{obs}(t - 1)$  has to be fulfilled. Of course, such “stretching” does not occur in reality, but  
 also in the  $\Delta$ SNOW.MODEL it is an infrequent case that only acts at a small scale. In any case the “stretching” is smaller than  
 255  $\tau$ . The issue is accepted as a model artifact, not least, because the “stretching” enables the very valuable adjustment to  $HS_{obs}$   
 at every point in time without forcing mass gains for insignificant  $HS$  raises within the measurement accuracy.

In case the density of an individual layer exceeds  $\rho_{max}$  by the scaling process, the excess mass is distributed layerwise from  
 top to bottom.  $SWE$  remains constant during scaling, unless it would be necessary to compact all layers beyond  $\rho_{max}$ . In

260 this case the appropriate excess mass is taken from the model-snowpack and interpreted as runoff,  $SWE$  is reduced and all layer thicknesses are cut accordingly (see *Runoff submodule* in Sect. 2.2.3 for details). As  $\tau$  turns out to be – reasonably and preferably – chosen in the order of a few centimeters (Sect. 3), the resulting reduction of  $SWE$  within the *Scaling module* is always quite small: e.g., with  $\tau = 2$  cm and maximum density chosen  $450 \text{ kg m}^{-3}$  (like Rohrer and Braun, 1994) the mass loss due to runoff is only  $9 \text{ kg m}^{-2}$ .

265 The *Scaling module* is illustrated as black arrows in Fig. 1. Note, the scaling is nothing “physical”, but also nothing “substantial” in terms of  $SWE$ , yet it is a smart way to utilize the advantage of having a measured snow depth at every point in time.

### 2.2.3 Drenching module

The *Drenching module*, finally, defines compaction due to liquid water percolating from top to bottom through the snowpack, loosening grain bonds and leading to densification (wet snow metamorphism). In case observed snow depth at a certain point in time is significantly lower than modeled snow depth ( $\Delta HS(t) < -\tau$ ), the *Drenching module* is activated.

The  $\Delta SNOW.MODEL$  ignores rain on snow since it concentrates on modeling  $SWE$  for pure snow depth records without having any further information on e.g. precipitation, temperature, snowfall level, etc. Possibilities how rain could be addressed in future developments are outlined in Sect. 4.

275 To cope with the model-observation-discrepancy  $\Delta HS(t) < -\tau$  the *Drenching module* densifies the model layers until  $\rho_{\max}$  is reached, starting from the uppermost one. Figuratively spoken, a certain layer gets drenched until saturation and meltwater is further distributed to the underlying layer. This process is repeated until (transient, therefore asterisked)  $HS^*$  equals  $HS_{\text{obs}}(t)$ . One or more layers might reach  $\rho_{\max}$ . In case  $\Delta HS(t)$  is so negative that all model snow layers are compacted and densified to  $\rho_{\max}$ , but still  $HS^* > HS_{\text{obs}}(t)$  the *Runoff submodule* is activated and runoff  $R(t)$  is defined as:

$$R(t) = (HS^* - HS_{\text{obs}}(t)) \cdot \rho_{\max}. \quad (6)$$

280 All layer thicknesses are “cut” by a respective portion:  $(HS^* - HS_{\text{obs}}) \cdot \frac{hs_i^*}{HS^*}$ . This mechanism does not reduce total number of layers, but layers potentially get very thin. During the melt season, where most of the runoff is produced, the *Runoff submodule* is more or less continuously active until  $HS_{\text{obs}}(t) = 0$  and all the snow has been converted to runoff. For a distinct snowpack from the first snow fall ( $t_1$ ) until getting snow-free again ( $t_2$ ) one has  $\sum_{t_1}^{t_2} R(t) = SWE_{\text{pk}}$ .

In Fig. 1 the *Drenching module* is shown by the brown and its *Runoff submodule* by the green arrows.

## 285 2.3 Calibration

The  $\Delta SNOW.MODEL$  has seven parameters that can be used for calibration:  $\rho_0$ ,  $\rho_{\max}$ ,  $\eta_0$ ,  $k$ ,  $\tau$ ,  $c_{\text{ov}}$ , and  $k_{\text{ov}}$  (cf. Tab. 3). For the first four parameters one finds suggestions and ranges in the literature:

Sturm and Holmgren (1998) do not address the criticality for the choice of new snow density, however, they use constant  $\rho_0 = 75 \text{ kg m}^{-3}$ . It is a well known characteristic of new snow to show large variations in densities. Helfricht et al. (2018) reviewed

290 many studies and give a general range of  $10 - 350 \text{ kg m}^{-3}$ , narrowing it down to “mean values” between  $70 - 110 \text{ kg m}^{-3}$ . Note, that this is daily densities. Sub-daily means of new snow densities are lower. Helfricht et al. (2018), for example, come up with an average of  $68 \text{ kg m}^{-3}$  for hourly time intervals. During the calibration process for the  $\Delta\text{SNOW.MODEL}$   $\rho_0$  was varied from 50 to  $200 \text{ kg m}^{-3}$ .

The second density-related calibration parameter is  $\rho_{\text{max}}$ , the maximum possible density within the model framework. As mentioned, Rohrer and Braun (1994) already set such a maximum at  $450 \text{ kg m}^{-3}$ . Also Sturm et al. (2010) defined it for five different climate classes, ranging from 217 to  $598 \text{ kg m}^{-3}$ . Glaciologists set the “critical density” before snow turns into firn to 400 to  $800 \text{ kg m}^{-3}$  (e.g., Paterson, 1998). Still, manual density measurements of seasonal snow used in previous studies hardly ever exceeded  $500 \text{ kg m}^{-3}$  (e.g., Jonas et al., 2009; Guyennon et al., 2019). Armstrong and Brun (2010) limit it to approximately 400 to  $500 \text{ kg m}^{-3}$  too. In order to find the fittest value for  $\rho_{\text{max}}$  used in the  $\Delta\text{SNOW.MODEL}$ , it was varied from 300 to  $600 \text{ kg m}^{-3}$ .

Equation (2) needs  $\eta_0$ , the “viscosity at [which]  $\rho$  equals zero” (Sturm and Holmgren, 1998). It is found to be in the order of  $8.5 \times 10^6 \text{ Pa s}$  (Sturm and Holmgren, 1998),  $6 \times 10^6 \text{ Pa s}$  (Jordan et al., 2010), and  $7.62237 \times 10^6 \text{ Pa s}$  (Vionnet et al., 2012). During the calibration process for the  $\Delta\text{SNOW.MODEL}$   $\eta_0$  was varied from 1 to  $20 \times 10^6 \text{ Pa s}$ . Parameter  $k$ , the second necessary parameter in Eq. (2), was varied from 0.011 to  $0.08 \text{ m}^3 \text{ kg}^{-1}$  by Sturm and Holmgren (1998) depending on climate region and respective different types of snow. However, they cite Keeler (1969) in their Table 2 with values for  $k$  for “Alpine-new” snow of up to  $0.185 \text{ m}^3 \text{ kg}^{-1}$ . In more complex snow models  $k$  is set to  $0.023 \text{ m}^3 \text{ kg}^{-1}$  (see Crocus:  $b_\eta$  in Vionnet et al. (2012)’s Equation (7); and also in Equation (2.11) of Jordan et al., 2010) or  $0.021 \text{ m}^3 \text{ kg}^{-1}$  (see SNTHERM: Equation (29) in Jordan, 1991). Its range for the  $\Delta\text{SNOW.MODEL}$  calibration was set from 0.01 to  $0.2 \text{ m}^3 \text{ kg}^{-1}$ .

There are no references for the latter three parameters. Threshold deviation  $\tau$ , as mentioned, might be interpreted as a measure of observation error, is regarded to be in the order of a few centimeters, and was modified from 1 cm to 20 cm for calibration. The last two parameters,  $c_{\text{ov}}$  and  $k_{\text{ov}}$ , determine the role of overburden strain and are newly introduced in the  $\Delta\text{SNOW.MODEL}$ . At least the limits of  $c_{\text{ov}}$  could be defined (Sect. 2.2.1) as  $c_{\text{ov}} \in \left[0, \min\left(\frac{1}{\sigma_0}\right)\right]$ .  $k_{\text{ov}}$  is only known to be a dimensionless, real, positive number. For calibrating the  $\Delta\text{SNOW.MODEL}$   $c_{\text{ov}}$  and  $k_{\text{ov}}$  were restrained by  $[0, 10^{-3} \text{ Pa}^{-1}]$  and  $[0.01, 10]$ , respectively.

315 The calibration performed in this study is based on  $\Delta t = 1 \text{ day}$ . Still, longer  $\Delta t$  (e.g., three days) as well as shorter  $\Delta t$  (e.g., one hour) are conceivable and could be handled by the  $\Delta\text{SNOW.MODEL}$ . Note, however, at least some calibration parameters will change significantly when changing  $\Delta t$ . This gets obvious when thinking about new snow density  $\rho_0$ , which of course is different if defined for one hour or for a three day timestep. The usage of this publication’s calibration parameters can, therefore, only be suggested for daily snow depth records.

### 320 2.3.1 Calibration Data and Method

The calibration process needs *SWE* data, but *SWE* measurements are quite rare (see Sect. 1). Furthermore, for calibration not only *SWE* observations are needed, but also regular snow depth records from the same places. Gruber (2014) collected 14 years of weekly *SWE* data from six stations in the Eastern Alps, measured by the observers of the Hydrographic Service

of Tyrol (Austria) between winters 1998/99 and 2011/12. The measurements of snow depth and water equivalent were made  
325 manually in snow pits with rulers and snow sampling cylinders ( $500\text{ cm}^3$ ), respectively. The sites range from 590 m to 1650 m  
altitude and are situated in relatively dry, inneralpine regions as well as in the Northern and Southern Alps, which are more  
humid due to orographic enhancement of precipitation (see Gruber, 2014, for details). The sites in the Southern Alps even  
show a moderate maritime influence due to their vicinity to the Mediterranean Sea, the most important source of moisture for  
this region (e.g., Seibert et al., 2007). These  $6 \times 14 = 84$  winter seasons cover 1166 measured  $HS-SWE$  pairs. Besides these  
330  $SWE$  measurements manual  $HS$  measurements are available for every day at the respective stations. Figure A1 and Table A1  
provide a map and a list, respectively.

The second source for  $SWE$  measurements used for calibration is Marty (2017). The Swiss SLF freely provides biweekly  
 $SWE$  and daily  $HS$  data from 11 stations in Switzerland. The  $HS$  measurements, accompanying the biweekly  $SWE$  mea-  
surements, were compared with the contemporary value of the daily  $HS$  records. Only those sites and years were used for  
335 calibration where the respective values of the daily  $HS$  record match the values of the biweekly measurements. If this con-  
dition is fulfilled, it is supposed that  $SWE$  and  $HS$  measurements fit together sufficiently well, although they unfortunately  
cannot always be taken exactly at the same place, which introduces uncertainty (e.g., López-Moreno et al., 2020). Conse-  
quently, 9 stations were used, most of them in the Northern Alps, some inneralpine, spanning an altitude range from 1200 m to  
1780 m, with all in all 56 winters and 388 pairs of  $HS$  and  $SWE$  measurements. Details are given in Fig. A1 and Table A1.  
340 Other stations and years suffer from discrepancies caused by too far distances between the measurements etc.

In order to ensure an unperturbed validation, the observation data sets from Austria and Switzerland (1554  $SWE - HS$   
pairs) were split in two almost equally big parts, one for model calibration ( $SWE_{cal}$ ) and one for validation ( $SWE_{val}$ ). The  
two data sources (Gruber, 2014; Marty, 2017) do not address the accuracy of the manual  $SWE$  observations. Mostly,  $SWE$   
measurements made with snow sampling cylinders are used as references in comparison studies, without addressing *their*  
345 accuracy (e.g., Sturm et al., 2010; Dixon and Boon, 2012; Kinar and Pomeroy, 2015; Leppänen et al., 2018). López-Moreno  
et al. (2020) provide a reported range of 3-13%, and condense the results of their own, very thorough and valuable experiments  
to an error range of 10-15% for bulk snow density. The majority of  $SWE_{cal}$  and  $SWE_{val}$  comes from the Hydrographic  
Service of Tyrol, Austria, where snow sampling cylinders ( $500\text{ cm}^3$ ) are used (Sect. 2.3.1). The repeatability of this kind  
of measurement is estimated at  $\pm 4\%$  for glacier mass balance studies (R. Prinz, Univ. of Innsbruck, Austria; pers. comm.).  
350 Roughly interpreting these density measurement “variabilities” as relative observation errors for  $SWE$ , the results for absolute  
accuracy would typically spread across the wide range of about 2 to  $50\text{ kg m}^{-2}$ .

Model calibration was performed with the statistical software  $R$  (R Core Team, 2019) and the  $R$  package *optimx* (Nash,  
2014). Results were obtained with optimization methods *L-BFGS-B* (Byrd et al., 1995) followed by *bobyqa* (Powell, 2009),  
which both are able to handle lower and upper bounds constraints. The function to be minimized was the root mean square  
355 error (RMSE) of  $SWE$ s from the  $\Delta$ SNOW.MODEL and observed  $SWE$ s, using the calibration data set  $SWE_{cal}$ .

### 3 Results

The following evaluates the ability of the  $\Delta$ SNOW.MODEL to calculate snow water equivalents exclusively from snow depths, and its practicability. Table 3 gives an overview of all parameters and summarizes the optimal setting for the  $\Delta$ SNOW.MODEL. A discussion of the best-fitted values and of the model sensitivity to parameter changes can be found in Sect. 4.

360 The minimal RMSE between all  $SWE$  observations used for calibration ( $SWE_{cal}$ ) and the respective modeled values is  $30.1 \text{ kg m}^{-2}$ . It is reached for new snow density  $\rho_0 = 81 \text{ kg m}^{-3}$ , maximum density  $\rho_{max} = 401 \text{ kg m}^{-3}$ , “viscosity parameters”  $\eta_0 = 8.5 \times 10^6 \text{ Pa}\cdot\text{s}$  and  $k = 0.030 \text{ m}^3 \text{ kg}^{-1}$ , threshold deviation  $\tau = 2.4 \text{ cm}$ , and “overburden parameters”  $c_{ov} = 5.1 \times 10^{-4} \text{ Pa}^{-1}$  and  $k_{ov} = 0.38$ .

#### 3.1 Validation and Comparison to other models

365 In this study no quantitative comparison with thermodynamic snow models was performed, since they need further meteorological data and the focus was on data records constrained to snow depths. However, the  $\Delta$ SNOW.MODEL was thoroughly evaluated against ERMs. Figure 2 and Table 4 show the results. Even though ERMs do not need meteorological data, it is not straight forward to calibrate them for new sites and applications. From the vast number of ERMs (cf. Avanzi et al., 2015) the ones of Pistocchi (2016) and Guyennon et al. (2019) were chosen to be fitted to  $SWE_{cal}$ . These models are quite new and easy  
370 to calibrate. Additionally, an approach simply using a constant bulk snow density at every point in time was calibrated to fit this study’s data.  $278 \text{ kg m}^{-3}$  turned out to be the optimal value minimizing root mean square errors of all  $SWE_{cal}$  values. Moreover, Jonas et al. (2009) and Sturm et al. (2010) were used for comparison. Unfortunately, calibration of these powerful models would have needed much more data than the 780  $SWE$ - $HS$ -pairs of the  $SWE_{cal}$  data set. Therefore, Jonas et al. (2009) and Sturm et al. (2010) were used with their standard parameters, but for Jonas et al. (2009) it was distinguished between regions  
375 (see Fig. 2’s caption). Other contemporary approaches had to be ignored, mostly because of the problematic transferability of regional parameters (e.g., McCreight and Small, 2014, or Mizukami and Perica, 2008).

The bias of modeled  $SWE$  (lower left panel in Fig. 2) is quite low and tendentially positive, meaning  $SWE$  is often slightly overestimated by the ERMs. The  $\Delta$ SNOW.MODEL slightly underestimates  $SWE$  on average, the median bias is  $-3.0 \text{ kg m}^{-2}$ . The overall good results for the ERMs is not particularly surprising, since they are dedicated to perform well *on average*.  
380 The specially calibrated versions of Pistocchi (2016) and Guyennon et al. (2019) show a significantly smaller bias than their originals. The model of Jonas et al. (2009) has the smallest bias for their “Region 7”, encompassing the dry, inneralpine Engadin as well as parts of the Southern Alps and the very East of Switzerland (Samnaun), which is partly influenced by orographic precipitation from Northwesterly flows. In terms of heterogeneity in precipitation climate “Region 7” is comparable to the region where the  $SWE$  data of this study comes from.

385 The other three indicators illustrated in Fig. 2 and summarized in Table 4 signify the better performance of the  $\Delta$ SNOW.MODEL compared to ERMs: The latter are intrinsically tied to snow depth (see Sect. 1.2) and are systematically forced to overestimate  $SWE_{pk}$ . Developers of ERMs are well aware of this, nevertheless,  $SWE_{pk}$  is probably the most-wanted snowpack feature in hydrology, climatology, and extreme value analysis. Note, the maximal  $SWE$  of a winter season not necessarily equals

the highest measured  $SWE$ , because measurements are only taken weekly or biweekly. In the vast majority of the  $SWE$  records used for this study, the highest seasonal observation is followed by at least one lower  $SWE$  reading. Sometimes real  $SWE$  might be higher after the highest measurement of a winter season was taken, but a thorough data check revealed, this is of minor importance here. It is sufficiently precise to assume that measured seasonal maximum  $SWE$  equals  $SWE_{pk}$ . The  $\Delta SNOW.MODEL$ 's bias of  $SWE_{pk}$  is very minor, only  $+0.3 \text{ kg m}^{-2}$ . Moreover, the  $\Delta SNOW.MODEL$  works better for the timing of  $SWE_{pk}$  (not shown in Fig. 2 and Table 4). ERM's tend to model  $SWE_{pk}$  some days too early, because the date of modeled  $SWE_{pk}$  is shifted towards the date of highest  $HS$  (cf. Fig. 4).

Another satisfactory validation result for the  $\Delta SNOW.MODEL$  is shown in Fig. 2's upper panels. RMSEs for all  $SWE$  values are constantly lower than if modeled with ERM's: a RMSE of  $30.8 \text{ kg m}^{-2}$  ( $\Delta SNOW.MODEL$ ) contrasts RMSEs between 39.1 and  $50.9 \text{ kg m}^{-2}$  (ERM's). Calibrating the models of Pistocchi (2016) and Guyennon et al. (2019) results in some improvement, at least they perform much better than the "constant density approach" after the calibration. The model of Jonas et al. (2009) does a decent job also without recalibration, which is remarkable. Sturm et al. (2010)'s method is calibrated with data from the Rocky Mountains. For this comparison the "alpine" parameters of Sturm et al. (2010) were taken, however, conditions might differ too much from the European Alps. Absolute errors in  $SWE$  increase with increasing  $SWE$ . For snowpacks lighter than  $75 \text{ kg m}^{-2}$   $\Delta SNOW.MODEL$  RMSE is  $17 \text{ kg m}^{-2}$ , between  $75 \text{ kg m}^{-2}$  and  $150 \text{ kg m}^{-2}$  it is  $26 \text{ kg m}^{-2}$ , and for snowpacks heavier than  $150 \text{ kg m}^{-2}$  it increases to  $43 \text{ kg m}^{-2}$ .

The  $\Delta SNOW.MODEL$  also has a small RMSE of  $36.3 \text{ kg m}^{-2}$  when modeling  $SWE_{pk}$  (Fig. 2, upper right; Table 4, last column). Also the  $SWE_{pk}$ -RMSEs for the different  $SWE$  classes are very close to those for  $SWE$ , which emphasizes the  $\Delta SNOW.MODEL$ 's ability to model all individual  $SWE$ 's comparably well. The evaluated ERM's have much higher, mostly at least doubled errors in simulated  $SWE_{pk}$ . Remarkably, the simple  $\rho_{278}$  approach is performing relatively well. In case the Jonas et al. (2009) model is suitably adjusted to regional specialties, it performs better than the other ERM's, but still significantly worse than the  $\Delta SNOW.MODEL$ .

The  $\Delta SNOW.MODEL$  outperforms empirical regression models. This can be argued on base of this study (especially Fig. 2), but even more when looking at the ERM studies themselves: Jonas et al. (2009) provide RMSEs between 50.9 and  $53.2 \text{ kg m}^{-2}$  for their standard model, which are quite high values compared to the findings of the study in hand ( $39.4 \text{ kg m}^{-2}$  for their Region 7, see Table 4). One explanation could be that Jonas et al. (2009) as well as other ERM studies rely on a huge amount of, but still diverse measurements in terms of record length, observations per season etc. The  $\Delta SNOW.MODEL$ -study only consists of data from selected stations with long and regular  $SWE$  readings, where also ERM's seem to work better. Guyennon et al. (2019) summarize their and other studies' validation results using MAE, the mean absolute error. Sturm et al. (2010) assess the bias for their "alpine" model at  $+29 \text{ kg m}^{-2}$  with a standard deviation of  $57 \text{ kg m}^{-2}$ , and they outline that "in a test against extensive Canadian data, 90% of the computed  $SWE$  values fell within  $\pm 80 \text{ kg m}^{-2}$  of measured values". Table 4 provides an overview and shows, that ERM's generally perform better with this study's data than with their original data.

## 3.2 Illustration

Figure 1 schematically shows the functioning of the  $\Delta$ SNOW.MODEL. A practical example is provided in Fig. 3, based on the optimal calibration parameters found during this study. Kössen, the station shown, is situated in the Northern Alps at 590 m above sea level (cf. Fig. A1). Although it is a low-lying place it is known to be snowy, which is, firstly, due to intense orographic enhancement of precipitation associated with Northwesterly to Northeasterly flows in the respective region (Wastl, 2008) and, secondly, comparably frequent inflow of cold continental air masses from Northeast. Showing Kössen should emphasize the versatile usability of the  $\Delta$ SNOW.MODEL: It is not only designed for high areas with deep, long-lasting snowpacks, but also for, e.g., valleys with shallow, ephemeral snowpacks. Winter 2008/09 was chosen because the  $\Delta$ SNOW.MODEL shows a rather typical performance in terms of RMSE and BIAS in Kössen then (see Table 4, values in brackets) and because some important, model-intrinsic features can be addressed and discussed:

Late November 2008 brought the first, however transient snowpack of the season (Fig. 3). The  $\Delta$ SNOW.MODEL identifies two days with snow fall (purple markings) and models two respective snow layers, which can be distinguished by the thin black line in Fig. 3. After about a week the snowpack starts to melt, the snow layers reach  $\rho_{\max}$  very fast (the blue shading gets dark), and finally all the snow was converted to runoff (green markings). In the second half of December there were three days with new snow, followed by a strong decline in snow depth. In the frame of the  $\Delta$ SNOW.MODEL this  $HS$  decrease is only possible, if the layers “get wet” and the *Drenching module* is activated (marked in brown). The layers get denser, starting at the top. However, the decrease was “manageable” by only increasing the two uppermost layer densities to  $\rho_{\max}$  and making the third layer just a bit denser. Not all layers got to  $\rho_{\max}$  (“saturated”) and no runoff was modeled. The  $\Delta$ SNOW.MODEL conserves the two dense layers until the end of the winter, which can clearly be seen in Fig. 3. One could interpret the layers as consisting of melt forms or a refrozen crust. However, interpretations like that require caution, because modeling such detailed layer features is not the intention of the  $\Delta$ SNOW.MODEL! During January Fig. 3 shows a phase where modeled values and observations agree to a high extent and only the *Scaling module* is activated for small adjustments (white markings). Small “stretching events” can be recognized, e.g. on January 2<sup>nd</sup> and 3<sup>rd</sup>, where model snow layers are set less dense in order to avoid too frequent mass gains. (This model behavior was thoroughly described in Sect. 2.2.2.) During continuous snowfalls in February the successive darkening of the blue layer shadings illustrates a phase of consequent compaction, which actually lasts until March, when strong decreases in  $HS_{\text{obs}}$  start to activate the *Drenching module*. Still, runoff is not yet produced. Only in the second half of March the whole model-snowpack reaches  $\rho_{\max}$  (“saturation”). The ablation phase is clearly distinguishable and lets the snowpack vanish quite fast until about April 10<sup>th</sup>, 2009.

The snow depth record of Kössen from 2008/09 was also used to compare different ERM and the  $\Delta$ SNOW.MODEL to  $SWE$  observations (Fig. 4). These measurements (light blue circles) are part of the  $SWE_{\text{val}}$  sample and were manually made with snow sampling cylinders; one after the December 2008 snowfall, and another nine on a nearly weekly base between late January and late March 2009. Figure 4 also provides various model results and some respective key values are given in Table 4. Not surprisingly, thus evidently, the ERM’s  $SWE$  curves “follow” the snow depth curve (black dashed line). The  $\Delta$ SNOW.MODEL (red line) does not get the first four measurements decently correct, the ERM performs better in this illustrative case. But after

455 the stronger snowfalls of February the picture changes indisputably in favor of the  $\Delta$ SNOW.MODEL. This is a typical pattern,  
nothing special for Kössen 2008/09, albeit it is quite pronounced in this example: The ERMs are too strongly tied to snow depth  
and, therefore, mostly (1) overestimate  $SWE_{pk}$ , (2) model its occurrence too early, and (3) – most importantly – force modeled  
 $SWE$  to reduce during pure compaction phases after snowfalls. Evidently, the ability of the  $\Delta$ SNOW.MODEL to “conserve”  
mass during the phases with dry metamorphism is its strongest point, not only in Kössen 2008/09 but also on average (cf. Fig.  
460 2 and Table 4).

## 4 Discussion and Outlook

Model results clearly depend on the parameters. Their optimal values are subject to calibration. The choice of the best-fitted  
values is rated and discussed in the following Sects. 4.1 to 4.5. Sections 4.6 to 4.8 cover possible future developments, accuracy  
issues, and the  $\Delta$ SNOW.MODEL’s applicability in remote sensing.

### 465 4.1 New Snow Density $\rho_0$

Being aware of both – the huge possible variations of new snow density depending on meteorological conditions during  
snowfalls and the possible cruciality of this parameter for  $SWE$  simulation by the  $\Delta$ SNOW.MODEL –  $\rho_0$  was chosen to be a  
constant in the framework of the model.  $\rho_0 = 81 \text{ kg m}^{-3}$  turned out to be the best choice after calibration with  $SWE_{cal}$ . This  
value clearly lies within the broader frame of possible new snow densities (Table 3) and quite closely to Sturm and Holmgren  
470 (1998)’s  $75 \text{ kg m}^{-3}$ , but it is found in the lower part for “typical” new snow densities (e.g., Helfricht et al., 2018). A possible  
explanation could be that the  $SWE$  measurement records used for the calibration tend to underrepresent late winter and spring  
conditions. Regular (weekly, biweekly) observations capture the short melt seasons worse than the longer accumulation phases.  
Therefore,  $SWE$  records might be biased towards early and mid winter new snow densities, which are lower (e.g., Jonas et al.,  
2009). Still, there are also some indications that using, e.g.,  $100 \text{ kg m}^{-3}$  as constant new snow density when modeling  $SWE$   
475 results in an overestimation of precipitation (up to 30% according to Mair et al., 2016). The calibrated value for  $\rho_0$  can be  
regarded as a reasonable result, even more when only considering it as a model parameter but not as a physical constant.

The sensitivity analysis illustrated in Fig. 5 confirms the importance of a good choice of  $\rho_0$ . Increasing  $\rho_0$  quite fast leads to  
a decrease of the relative bias of seasonal  $SWE$  maxima ( $SWE_{pk}$ ). Note the definition of the relative bias in Fig. 5’s caption.  
In absolute values: too small  $\rho_0$  cause too small  $SWE_{pk}$ , using higher values leads to an overestimation of  $SWE_{pk}$ . This  
480 behavior supports above-mentioned tendency to overestimate precipitation when choosing constant  $100 \text{ kg m}^{-3}$  as new snow  
density. As expected, the new snow density is the most crucial parameter of the  $\Delta$ SNOW.MODEL (cf. Table 3). The median  
relative bias of  $SWE_{pk}$  changes by  $-0.46\%$  per  $+1 \text{ kg m}^{-3}$ , if the whole calibration range of  $\rho_0$  is considered to calculate the  
sensitivity ( $50 - 200 \text{ kg m}^{-3}$ ). This means a median change in  $SWE_{pk}$  of  $+0.37 \text{ kg m}^{-2}$  when  $\rho_0$  is risen by  $+1 \text{ kg m}^{-3}$ . If  
the limits are chosen tighter around the optimal value, the gradient is even steeper:  $-0.62\%$  and  $+0.50 \text{ kg m}^{-2}$  per  $+1 \text{ kg m}^{-3}$ ,  
485 respectively, when the gradient is approximated for the range  $70 - 90 \text{ kg m}^{-3}$ . Widely-used  $\rho_0 = 100 \text{ kg m}^{-3}$ , consequently,  
causes a median overestimation of  $SWE_{pk}$  of about 12% in the  $\Delta$ SNOW.MODEL. Daily  $SWE$  show the same behavior (not



shown). Users should be aware of this. The suggestion clearly is to either use the best-fitted parameters of this study or recalibrate *all* parameters with appropriate *SWE* data, but not adjusting only single parameters. As the calibration data of this study are spread across various climates and altitudes, users can be quite confident to get good results if using  $\rho_0 = 81 \text{ kg m}^{-3}$ .  
490 This value seems to be a good compromise, at least at alpine areas. However, for very maritime, very dry, polar or tundra regions the optimized  $\rho_0$  should be used with caution; if possible, recalibration is recommended.

## 4.2 Maximum Density $\rho_{\max}$

Of course, the maximum bulk snow density of a snowpack changes from year to year and site to site. For the  $\Delta\text{SNOW.MODEL}$  simplicity and independence from meteorological variables outweigh precision. Even more so, when there are good arguments  
495 for the existence of a “typical” maximum bulk density  $\rho_{\max}$ . Put simply, (not too old) seasonal and also ephemeral snowpacks melt away when they get water saturated. Before that, there is limited time for dry densification; dry winter snow’s bulk density is widely described as staying below about  $350 \text{ kg m}^{-3}$  (e.g., Paterson, 1998; Sandells et al., 2012). Accounting for the fact that volumetric liquid water content of about 10% marks the funicular mode of liquid distribution in old, coarse-grained snow (Denoth, 1982; Mitterer et al., 2011), this leads to the rough estimate of a typical maximum bulk density of about  
500  $\frac{9}{10} \cdot 350 + \frac{1}{10} \cdot 1000 = 415 \text{ kg m}^{-3}$ . Convincingly, the fittest value for  $\rho_{\max}$  in the  $\Delta\text{SNOW.MODEL}$  turns out to be  $401 \text{ kg m}^{-3}$ , which is close to that value and well situated within the range given in the literature (Table 3). Moreover, this is virtually the same value like the median maximum seasonal density of the *SWE*<sub>val</sub> data records ( $400 \text{ kg m}^{-3}$ , see box plot in Fig. 6), another indication why  $\rho_{\max}$  could be regarded as a typical seasonal maximum of  $\rho_b$ .

Figure 5 illustrates the similarity between  $\rho_0$  and  $\rho_{\max}$  regarding their influence on *SWE* simulations. Keeping the other  
505 six  $\Delta\text{SNOW.MODEL}$  parameters constant but increasing  $\rho_{\max}$  leads to increased *SWE*<sub>pk</sub> and vice versa – just like  $\rho_0$ . This is not surprising, however reasonable. The  $\Delta\text{SNOW.MODEL}$  is not as sensitive to changes in  $\rho_{\max}$  than to changes in  $\rho_0$ : Raising  $\rho_{\max}$  by  $+1 \text{ kg m}^{-3}$  leads to a mean decrease of the relative bias of *SWE*<sub>pk</sub> of  $-0.06\%$ , which corresponds to an increase in absolute *SWE*<sub>pk</sub> of  $+0.24 \text{ kg m}^{-2}$  per  $+1 \text{ kg m}^{-3}$ . The same argumentation like for  $\rho_0$  in Sect. 4.1 lets users of the  $\Delta\text{SNOW.MODEL}$  be quite sure when taking  $\rho_{\max} = 401 \text{ kg m}^{-3}$ , the best-fitted value according to this study’s calibration. Be  
510 aware that solely changing parameter  $\rho_{\max}$  for an application of the  $\Delta\text{SNOW.MODEL}$  elsewhere, without proper recalibration of the other parameters, might lead to significant changes in the results for *SWE*.

## 4.3 Viscosity Parameters $\eta_0$ and $k$

Equation (2) represents the settlement and densification function of the  $\Delta\text{SNOW.MODEL}$ . Two parameters  $\eta_0$  and  $k$  act as adjustment screws and have to be calibrated. In this study best-fitted  $\eta_0$  is  $8.5 \times 10^6 \text{ Pa s}$  and the optimized value for  $k$  is  
515  $0.030 \text{ m}^3 \text{ kg}^{-1}$ . Both values are close to other studies’ results and suggestions (Table 3).

As far as the  $\Delta\text{SNOW.MODEL}$ ’s sensitivity to changes in the “viscosity parameters”  $\eta_0$  and  $k$  is concerned, Fig. 5 shows that an isolated rise of the model snow viscosity – either by enhancing  $\eta_0$  or  $k$  – increases the relative bias of *SWE*<sub>pk</sub>, which means a decrease in absolute values of *SWE*<sub>pk</sub>. This behavior is consistent, since higher viscosity reduces the densification rate and the model-snowpack tendentially stays deeper. Consequently, increases in observed snow depth tend to bring less new snow

520 while the *New Snow module* is run (Sect. 2.2.1). Finally, simulated  $SWE_{pk}$  is reduced when  $\eta_0$  or  $k$  are increased and vice versa.

#### 4.4 Threshold Deviation $\tau$

The  $\Delta$ SNOW.MODEL's parameter to cope with uncertainties in snow depth is  $\tau$ . It is supposed to be not bigger than a few centimeters. In particular, it should avoid excessive production of snow mass in the model through too frequent simulation of  
525 new snow events (see Sect. 2.2).  $\tau$  is kind of a peculiarity of the  $\Delta$ SNOW.MODEL and therefore no bounds can be found in literature. It was generously accepted to range between 1 and 20 cm for calibration and turned out to be optimal at  $\tau = 2.4$  cm (Table 3). Given the wide range of possible values, this is very close to what it would be expected to be as a measure for  $HS_{obs}$  accuracy.

Model sensitivity to changes in  $\tau$  turns out to be quite low for values in the order of a few centimeters, but the influence on  
530 simulated  $SWE_{pk}$  is strongly increasing if  $\tau$  is chosen greater than about 5 cm (Fig. 5). This result makes a lot of sense, if  $\tau$  is seen as a measure of observation accuracy, because this is very likely to be better than 5 cm. Like changes in  $\eta_0$  and  $k$ , changes in  $\tau$  are indirect proportional to changes in  $SWE_{pk}$ , for a closely related reason: The bigger  $\tau$  the more often small new snow events are not counted as such because the *Scaling module* (Sect. 2.2.2) is more frequently activated at the cost of the *New Snow module* (Sect. 2.2.1). Mass gains are tendentially modeled less frequently and, as a consequence, snow water equivalents  
535 get smaller.

#### 4.5 Overburden Parameters $c_{ov}$ and $k_{ov}$

Aside  $\tau$ , there are two more parameters that are peculiar to the  $\Delta$ SNOW.MODEL. They are needed to simulate unsteady compaction by overburden load of new snow. Because of their presumed uniqueness in the snow model spectrum there is no information available on how to choose them (see Sect. 2.3). However, the calibration produces  $c_{ov} = 5.1 \times 10^{-4} \text{ Pa}^{-1}$  and  
540  $k_{ov} = 0.38$  as fittest values (Table 3).

As outlined in Sect. 2.2.1, the implementation of overburden strain in the  $\Delta$ SNOW.MODEL is supposed to be an important aspect of the model. Still, the sensitivity of modeled  $SWE_{pk}$  to changes in either  $c_{ov}$  or  $k_{ov}$  are quite minor. (See Fig. 5 for  $c_{ov}$ .  $k_{ov}$  is not shown, because it is comparable, but with different sign.) The reason for this relative insensitivity of the model to changes in  $c_{ov}$  and  $k_{ov}$  could be the contradicting effects of these two “overburden parameters”: Higher  $c_{ov}$  push overburden  
545 strain  $\epsilon$  towards 1.0 (cf. Eq. (3)), which increases the role of overburden snow.  $hs^*$  and  $HS^*$  of Eq. (4) are reduced and, consequently, the new layer thickness and mass are increased (Eq. (5)). Higher  $c_{ov}$ , therefore, lead to higher  $SWE$  and  $SWE_{pk}$ . For  $k_{ov}$  it is the opposite, higher values of  $k_{ov}$  cause lower  $SWE$ .

#### 4.6 Incorporating Rain-on-Snow and other possible improvements

In principle, the  $\Delta$ SNOW.MODEL could deal with rain-on-snow events. Unsteady compaction due to overburden load, for exam-  
550 ple, is not restricted to new snow. It could also be triggered by the mass of rain water – in nature, but also in the framework of the

$\Delta$ SNOW.MODEL. Still, the respective feature is not implemented at the moment, because identifying criteria for rain-on-snow events based on pure snow depth records is very problematic, and its resolving is beyond the scope of this paper. In case meta information on rain climate or on precipitation type and amount is available, it could be incorporated in the  $\Delta$ SNOW.MODEL. Given the relative success of the  $\Delta$ SNOW.MODEL in its current version the probably very costly, but potentially often only very  
555 minor improvements when including rain-on-snow should be considered.

Another eventual future development is the refinement of the density parameters  $\rho_0$  and  $\rho_{max}$  since, firstly, the  $\Delta$ SNOW.MODEL reacts quite sensitive on their changes and, secondly, some relations are well known, e.g.,  $\rho_0$ 's dependence on the climatic aridness or  $\rho_{max}$ 's tendentious increase for aging snow. Setting  $\rho_{max}$  to a fixed value at about  $400 \text{ kg m}^{-3}$  actually disqualifies the  $\Delta$ SNOW.MODEL for snow older than estimated 200 days. Additional calibrations could be performed for very maritime, very  
560 dry, polar, or tundra regions as well as for very long-lasting snowpacks. Note, however, all of these adaptations introduce more parameters to the  $\Delta$ SNOW.MODEL and reduce its generality. Benefits should be evaluated critically, and probably this evaluation should start with the overburden load treatment of the  $\Delta$ SNOW.MODEL. It is possible that refining the density parameters is more valuable than the special treatment of unsteady compaction due to overburden loads.

#### 4.7 SWE Accuracy

565 Table 4 provides an overview of uncertainties for *SWE*, also for thermodynamic models: Vionnet et al. (2012) find a ~~root mean square error~~ and bias of  $39.7 \text{ kg m}^{-2}$  and  $-17.3 \text{ kg m}^{-2}$ , respectively, comparing 1722 manual samplings at Col de Porte (Chartreuse Mountains, France) and Crocus. Wever et al. (2015) and Sandells et al. (2012) come up with RMSEs of about  $39.5 \text{ kg m}^{-2}$  (SNOWPACK) and  $30 - 49 \text{ kg m}^{-2}$  (SNOBAL), respectively. Langlois et al. (2009) find more optimistic values, however, based on much fewer data. On the contrary, Egli et al. (2009) give reason to expect higher RMSEs, but their  
570 study exclusively bases on data from  $\Delta$ snowy, high altitude station Weissfluhjoch (Switzerland), which intrinsically promotes higher absolute errors. Essery et al. (2013)'s comprehensive simulation experiment results in a RMSE-range of  $23 - 77 \text{ kg m}^{-2}$ .

As a synopsis of the study in hand, absolute *SWE* accuracies could be estimated as follows: (1) 2 to  $50 \text{ kg m}^{-2}$  for manual measurements, which are widely used as reference, (2) 30 to  $40 \text{ kg m}^{-2}$  for thermodynamic models, and (3) 40 to  $50 \text{ kg m}^{-2}$  for empirical regression models. In this respect, it is striking to find the  $\Delta$ SNOW.MODEL's RMSE at  $30.8 \text{ kg m}^{-2}$ .

#### 575 4.8 Application to Remote Sensing Data

Looking at current developments in deriving *SWE* from snow depths monitored with lidar and photogrammetry, the  $\Delta$ SNOW.MODEL should be considered as one of the "potential [...] other snow density models" (Smyth et al., 2019) that should be included in respective future research. Lidar and photogrammetry have errors in the order of 10 cm (Smyth et al., 2019), typically corresponding to *SWE* errors of 20 to  $40 \text{ kg m}^{-2}$ . This is in the order of the  $\Delta$ SNOW.MODEL errors. Remote sensing derived  
580 snow depth data are discontinuous through time. The  $\Delta$ SNOW.MODEL would have to be adapted to that, but for the benefit of upgrading the  $\Delta$ SNOW.MODEL from a point model to a computationally fast distributed model.

## 5 Conclusions

A new method to simulate snow water equivalents (*SWEs*) is presented. It exclusively needs snow depths and their temporal changes as input, which is its major advantage compared to many other snow models. It is shown that basic snow physics, smartly implemented in a layer model, suffice to better calculate *SWE* than snow models relying on empirical regressions.

Regular snow depth records are used to stepwise model the evolution of seasonal snowpacks, focusing on their mass (i.e. *SWE*) and respective load. Snow compaction is assumed to follow Newtonian viscosity, unsteady stress for underlying snow layers by the overburden load of new snow is regarded separately, melted mass is distributed from upper to lower layers, and – eponymous for the model – the measured change in snow depth between two observations is used as a precious corrective, though by accounting for measurement uncertainties.

The  $\Delta$ SNOW.MODEL mainly bases on Martinec and Rango (1991) and Sturm and Holmgren (1998), and transforms them to a modern R-code, which is available through <https://cran.r-project.org/package=nixmass>. Aside snow depth, meteorological and also geographical input is consequently avoided in the framework of the  $\Delta$ SNOW.MODEL. Still, calibration of seven parameters is needed. To provide an optimal setting and utmost applicability, data from 14 climatologically different places in the Swiss and Austrian Alps are utilized. This is challenging, since calibration needs multi-year *SWE* observations as well as consecutive (e.g. daily) snow depth readings from the same places. The  $\Delta$ SNOW.MODEL is calibrated with 67 winters. The validation data set consists of another 71 independent winters. Whereas calibration is rather complex, the application of the  $\Delta$ SNOW.MODEL is cheap in terms of computational effort: Deriving a one-year *SWE* record from 365 snow depth values, e.g., only takes a few seconds with today's standard desktop CPUs and can certainly be speeded up significantly.

In this study it is argued that the  $\Delta$ SNOW.MODEL is situated between sophisticated “thermodynamic snow models”, necessitating lots of meteorological and other input, and modest “empirical regression models” (ERMs), relying on statistical relations between *SWE* and snow depth, date, altitude, and region. These key qualities of the  $\Delta$ SNOW.MODEL are:

- low complexity: The  $\Delta$ SNOW.MODEL is a semi-empirical multi-layer model with seven parameters. It only needs regular *HS* records as input. In some respect it is even less demanding than ERMs, because no information on date, altitude, or region is required.
- high universality: The  $\Delta$ SNOW.MODEL simulates individual *SWE* values – like the important seasonal maximum  $SWE_{pk}$  – comparably well as *SWE* averages.
- high accuracy: The  $\Delta$ SNOW.MODEL's performance in modeling *SWE* and  $SWE_{pk}$  is comparable to thermodynamic models and superior to ERMs. Root mean square errors for  $SWE_{pk}$  are  $36.3 \text{ kg m}^{-2}$  for the  $\Delta$ SNOW.MODEL and about 70 to  $> 100 \text{ kg m}^{-2}$  for ERMs.

The development of the  $\Delta$ SNOW.MODEL is application-driven. It is therefore not surprising that this study provides no significant new findings in snow physics. Still, the  $\Delta$ SNOW.MODEL seems to be the first model since long that takes well known basic snow principles and arranges them in a physically consistent way, while consequently ignoring all potential information except snow depth. Not particularly innovative, but remarkably successful. The  $\Delta$ SNOW.MODEL is widely usable,

615 but first of all it can attribute snow water equivalents to all longterm and historic snow depth records, which are so valuable for climatological studies and extreme value analysis for risk assessment of natural hazards .

*Code availability.* R-code of the  $\Delta$ SNOW.MODEL and some empirical regression models: <https://cran.r-project.org/package=nixmass>. (Python-code of the  $\Delta$ SNOW.MODEL, ported by M. Theurl (Univ. of Graz, Austria): [https://bitbucket.org/atraxoo/snow\\_to\\_swe](https://bitbucket.org/atraxoo/snow_to_swe).)

## Appendix A

620 A map with the stations used for calibration and validation of the  $\Delta$ SNOW.MODEL is shown in Fig. A1. Table A1 provides details on the stations and the data.

## Appendix B

625 The *Scaling module* (Sect. 2.2.2) recalculates the “viscosity parameter”  $\eta_0$ . This temporary  $\eta_0^*(i, t)$  does not only depend on the point in time  $t$  whenever the *Scaling module* is activated, but is also different for each layer  $i$ . The reason is described in the following.

The *Scaling module* aims for the condition, that today’s model snow depth  $HS(t)$  equals today’s observed snow depth  $HS_{\text{obs}}(t)$ .

$$HS(t) = \sum_{i=1}^{ly(t)} hs(i, t) \stackrel{!}{=} HS_{\text{obs}}(t)$$

It follows from Eq. (2) and substituting  $x(i, t) = \Delta t \cdot \hat{\sigma}(i, t) \cdot e^{-k \cdot \rho(i, t)}$ :

$$\sum_{i=1}^{ly(t)} hs(i, t) = \sum_{i=1}^{ly(t)} \frac{\eta_0^*(t) \cdot hs(i, t-1)}{\eta_0^*(t) + x(i, t)} \stackrel{!}{=} HS_{\text{obs}}(t), \quad (\text{B1})$$

which is a rational function  $f$  of the form

$$f(\eta) = \sum_{i=1}^N \frac{\eta \cdot h_i}{\eta + x_i}$$

630 Because  $f(\eta)$  has poles at  $-x_1, \dots, -x_N$ , the equation  $f(\eta) = HS_{\text{obs}}$  has multiple solutions. Consequently, this approach – with  $\eta_0^*(t)$  being independent from layer  $i$  – shows a clear non-physical behavior making it necessary to calculate different  $\eta_0^*(i, t)$  for each layer  $i$  based on Eq. (B1):

$$\eta_0^*(i, t) = \frac{x(i, t) \cdot hs(i, t)}{hs(i, t-1) - hs(i, t)}$$

The solution of this issue in the *Scaling module* of the  $\Delta$ SNOW.MODEL bases on the assumption, that observed compaction between  $t - 1$  and  $t$  can be approximated linearly for each layer:

$$\frac{hs(i, t)}{hs(i, t - 1)} \stackrel{!}{\approx} \frac{HS_{\text{obs}}(t)}{HS_{\text{obs}}(t - 1)}$$

635 The layer-individual viscosities can be calculated as

$$\eta_0^*(i, t) = \frac{x(i, t) \cdot HS_{\text{obs}}(t)}{HS_{\text{obs}}(t - 1) - HS_{\text{obs}}(t)}$$

Substituting those values for  $\eta_0^*$  in Eq. (B1) fulfills its precondition, and the modeled equals the observed snow depth. The newly calculated  $\eta_0^*(i, t)$  are different for each layer – in contrast to the fixed  $\eta_0$  defined in Sect. 2.1, which is valid for the whole snowpack (outside the *Scaling module*). Note, these new viscosities are only used temporarily in the *Scaling module*. They have no analog in reality and can also have negative values, but they are mathematically sound.

## 640 Appendix C: Example of Application – Snow Load Map of Austria

In this section an example is given how the  $\Delta$ SNOW.MODEL can be used to attain a map of snow loads in Austria. European Standards (e.g., European Committee for Standardization, 2015) define the “characteristic snow load”  $s_k$  as the weight of snow on the ground with an annual probability of exceedance of 0.02, i.e. a snow load that – on average – is exceeded only once within 50 years. Unfortunately, *SWE* is not measured on a regular basis at a reasonable number of sites in Austria (and most  
645 other countries). The  $\Delta$ SNOW.MODEL, however, can provide longterm Austrian *SWE* series from widely available *HS* series, which can in turn be used for a spatial extreme value model. No other snow model is capable of this in a comparable manner, since either  $SWE_{\text{pk}}$  is poorly modeled (ERMs) or more meteorological input would be needed (thermodynamic models). Among several possibilities to spatially model snow depth extremes like max-stable processes (see e.g. Blanchet and Davison, 2011), the *smooth modeling* approach of Blanchet and Lehning (2010) can be used when marginals instead of spatial extremal  
650 dependence is in focus.

### C1 Smooth Modeling

Extremes following a generalized extreme value distribution (GEV; Coles, 2001) with parameters  $\mu$ ,  $\sigma$  and  $\xi$  can be modeled in space by considering linear relations for the three parameters of the form

$$\eta(x) = \alpha_0 + \sum_{k=1}^m \alpha_k y_k(x) \tag{C1}$$

655 at location  $x$ , where  $\eta$  denotes one of the GEV parameters,  $y_1, \dots, y_m$  are the considered covariates as smooth functions of the location, and  $\alpha_0, \dots, \alpha_m \in \mathbb{R}$  are the coefficients. Assuming spatially independent stations, the log-likelihood function then reads as

$$l = \sum_{k=1}^K \ell_k(\mu(x_k), \sigma(x_k), \xi(x_k)), \quad (\text{C2})$$

660 where  $l$  only depends on the coefficients of the linear models for the GEV parameters. This approach was termed *smooth modeling* by Blanchet and Lehning (2010). A smooth spatial model for extreme snow depths in Austria was already presented in Schellander and Hell (2018), using longitude, latitude, altitude, and mean snow depth at 421 stations. Considering the strong correlation between snow depth and snow water equivalent, it would be natural to spatially model *SWE* extremes in the same manner.

## C2 Fitting a Spatial Extreme Value Model

665 For this application 214 stations with regular snow depth observations in and tightly around Austria of the National Weather Service (ZAMG) and the Hydrological Services are used. The dataset has undergone quality control by the maintaining institutions and covers altitudes between 118 and 2290 m. The records have lengths of 43 years and cover winters from 1970/71 to 2011/2012.

670 In a first step the  $\Delta$ SNOW.MODEL was applied to these snow depth series to achieve 214 data series of *SWE* across Austria. Then the linear models for the three GEV parameters according to Sect. C1 were defined via a model selection procedure. For that purpose a generalized linear regression was performed between the parameters and the covariates longitude, latitude, altitude, and mean snow depth, which were added in a stepwise manner. Using the Akaike information criterion (AIC; Akaike, 1974), the best linear model between a given full model ( $\mu \sim$  all covariates) and a null model ( $\mu \sim 1$ ) with the smallest AIC was selected. Using these models and the covariates of the 214 stations, a smooth spatial model for the yearly maxima of the *SWE* values was fitted.

## C3 Return Level Map of 50-year Snow Load in Austria

680 The spatial extreme value model developed in the previous section was applied to a grid provided by the SNOWGRID climate analysis (Olefs et al., 2013). It offers the necessary covariates longitude, latitude, altitude, and yearly mean snow depths from 1961 to 2016. The grid features a horizontal resolution of  $1 \times 1$  km. Some minor SNOWGRID pixels have unrealistically large mean snow depth values, arising from a poor implementation of lateral snow redistribution at high altitudes (18 pixels, i.e. 0.02% with values between 5 and 65 m). They are masked for the calculation of *SWE* return level maps. The return level map for a return period of 50 years can be seen in Fig. A2.

As expected, due to the strong correlation of the *SWE* maxima with mean snow depth, the largest snow loads are located in the mountainous areas of Austria. Although the unrealistic mean snow depth values of SNOWGRID are masked, the

685 model produces a number of 59 (0.06%) unrealistic snow load values larger than  $25 \text{ kN m}^{-2}$  in an altitude range between 1500 and 3700 m. For a model that would be seriously used e.g. in general risk assessment or structural design, this problem could possibly be tackled with a non-linear relation between *SWE* maxima and mean snow depth or altitude. This is, however, beyond the scope of this study. Note, that in the actual Austrian standard (Austrian Standards Institute, 2018) there are no normative snow load values defined above 1500 m altitude.

690 All but two locations of the Austrian *SWE* measurement series that were used for calibration *and* validation of the  $\Delta\text{SNOW.MODEL}$  (see Sect. 2.3.1) are included in the dataset used to fit the spatial model in Sect. C2. Those two stations, Holzgau and Felbertauern with 14 years of *SWE* observations each, are used to qualitatively compare (1) the spatial model fitted in Sect. C2, (2) *SWE* extremes modeled from daily snow depths with the  $\Delta\text{SNOW.MODEL}$ , and (3) extremes computed “directly” from (ca. weekly) observed *SWE* values. Figure A3 gives an idea of the model performance at stations Holzgau and Felbertauern  
695 (see Figs. A1 and A2 for their locations). For the lower-lying station Holzgau (1100 m) all three variants overlap very well. The 50-year return level is  $4.65 \text{ kN m}^{-2}$  for the smooth spatial model,  $4.72 \text{ kN m}^{-2}$  for the  $\Delta\text{SNOW.MODEL}$ , and  $4.8 \text{ kN m}^{-2}$  for the observations. Note, that the latter stem from weekly observations and, therefore, not necessarily reflect the true yearly maxima, which naturally must be equal or slightly higher. By the way, the corresponding value of  $s_k$  from the Austrian snow load standard for Holzgau is  $6.3 \text{ kN m}^{-2}$  (Austrian Standards Institute (2018); accessible online at eHORA (2006)).

700 For the higher station Felbertauern (1650 m) the agreement between *SWE* from the  $\Delta\text{SNOW.MODEL}$  and observed values is again very good. However, their GEV fits differ significantly. While the fit to the observations shows a negative shape parameter of  $\xi = -0.1$ , the fit to the values modeled with the  $\Delta\text{SNOW.MODEL}$  gives a positive shape parameter of  $\xi = 0.1$ , leading to much larger return levels for higher recurrence times. It should be pointed out that the GEV fits based on  $\Delta\text{SNOW.MODEL}$  simulations and observations are unreliable, given the short data sample of only 14 yearly maxima. Indeed, by using a sample  
705 size of 43 years and borrowing strength from neighboring stations, the spatial model provides the best fit to observations as well as modeled *SWE* values. The 50-year snow load return values are  $6.4 \text{ kN m}^{-2}$  for the spatial model,  $6.8 \text{ kN m}^{-2}$  for the  $\Delta\text{SNOW.MODEL}$ , and  $5.7 \text{ kN m}^{-2}$  for the fit to the observations. No normative value is defined for Felbertauern because it is situated higher than 1500 m (Austrian Standards Institute, 2018).

*Author contributions.* MW rose and led the project, structured and managed it. He was a key figure in developing and designing the snow  
710 model, and he did most of the writing. HS developed, coded and calibrated the model. He wrote the R-package and helped writing the paper, particularly the application example in the appendix. SG developed early versions of the model and its code.

*Competing interests.* The authors declare no competing interests.



715 *Acknowledgements.* The authors want to acknowledge T. Hell (Dept. of Mathematics, Univ. of Innsbruck, Austria) who substantially helped with the *Scaling module* (Sect. 2.2.2 and Appendix B). Thanks also go to the Hydrographic Service of Tyrol (Austria) which provided part of the data. A. Radlherr and J. Staudacher (ZAMG, Austria) is thanked for vivid discussions and proof-reading. Not least, we want to acknowledge M. Theurl and J. Abermann from the Univ. of Graz (Austria) for porting the  $\Delta$ SNOW.MODEL's R-code to Phyton.

*Financial support.* This work was embedded in the project "Schneelast.Reform", funded by the Austrian Research Promotion Agency (FFG) and the Austrian Economic Chamber (WKO), in particular by their Association of the Austrian Wood Industries (FV Holzindustrie).

720 *Review statement.* This paper was edited by Markus Weiler and reviewed by three anonymous referees. The authors highly appreciate their comments and suggestions since they significantly improved the manuscript.

## References

- Akaike, H.: A new look at the statistical model identification, *IEEE Transactions on Automatic Control*, 19, 716–723, <https://doi.org/10.1109/TAC.1974.1100705>, 1974.
- Armstrong, R. L. and Brun, E.: *Snow and climate: physical processes, surface energy exchange and modeling*, Cambridge University Press, Cambridge, 2010.
- Austrian Standards Institute: ÖNORM B 1991-1-3:2018-12-01, 2018.
- Avanzi, F., De Michele, C., and Ghezzi, A.: On the performances of empirical regressions for the estimation of bulk snow density, *Geografia Fisica e Dinamica Quaternaria*, pp. 105–112, <https://doi.org/10.4461/GFDQ.2015.38.10>, 2015.
- Blanchet, J. and Davison, A.: Spatial modeling of extreme snow depth, *The Annals of Applied Statistics*, 5, 1699–1725, <https://doi.org/10.1214/11-AOAS464SUPP>, 2011.
- Blanchet, J. and Lehning, M.: Mapping snow depth return levels: smooth spatial modeling versus station interpolation, *Hydrology and Earth System Sciences*, 14, 2527–2544, <https://doi.org/10.5194/hess-14-2527-2010>, 2010.
- Byrd, R. H., Lu, P., Nocedal, J., and Zhu, C.: A Limited Memory Algorithm for Bound Constrained Optimization, *SIAM Journal on Scientific Computing*, 16, 1190–1208, <https://doi.org/10.1137/0916069>, 1995.
- Coles, S.: *An introduction to statistical modeling of extreme values*, Springer Series in Statistics, Springer-Verlag, London, 2001.
- De Michele, C., Avanzi, F., Ghezzi, A., and Jommi, C.: Investigating the dynamics of bulk snow density in dry and wet conditions using a one-dimensional model, *The Cryosphere*, 7, 433–444, <https://doi.org/10.5194/tc-7-433-2013>, 2013.
- Deems, J. S., Painter, T. H., and Finnegan, D. C.: Lidar measurement of snow depth: a review, *Journal of Glaciology*, 59, 467–479, <https://doi.org/10.3189/2013JoG12J154>, 2013.
- Denoth, A.: The Pendular-Funicular Liquid Transition and Snow Metamorphism, *Journal of Glaciology*, 28, 357–364, <https://doi.org/10.3189/S0022143000011692>, 1982.
- Dietz, A., Kuenzer, C., Gessner, U., and Dech, S.: Remote Sensing of Snow – a Review of available methods, *International Journal of Remote Sensing*, 33, 4094–4134, <https://doi.org/10.1080/01431161.2011.640964>, 2012.
- Dixon, D. and Boon, S.: Comparison of the SnowHydro snow sampler with existing snow tube designs, *Hydrological Processes*, 26, 2555–2562, <https://doi.org/10.1002/hyp.9317>, 2012.
- Egli, L., Jonas, T., and Meister, R.: Comparison of different automatic methods for estimating snow water equivalent, *Cold Regions Science and Technology*, 57, 107–115, <https://doi.org/https://doi.org/10.1016/j.coldregions.2009.02.008>, 2009.
- eHORA: Natural Hazard Overview & Risk Assessment Austria, <https://hora.gv.at/>, [Online; accessed 13-March-2020], 2006.
- Essery, R., Morin, S., Lejeune, Y., and Ménard, C. B.: A comparison of 1701 snow models using observations from an alpine site, *Advances in Water Resources*, 55, 131–148, <https://doi.org/https://doi.org/10.1016/j.advwatres.2012.07.013>, 2013.
- European Committee for Standardization: EN 1991-1-3:2003/A1:2015, 2015.
- Fierz, C., Armstrong, R., Durand, Y., Etchevers, P., Greene, E., McClung, D., Nishimura, K., Satyawali, P., and Sokratov, S.: The International Classification for Seasonal Snow on the Ground, *IHP-VII Technical Documents in Hydrology*, 83, <http://unesdoc.unesco.org/images/0018/001864/186462e.pdf>, 2009.
- Garvelmann, J., Pohl, S., and Weiler, M.: From observation to the quantification of snow processes with a time-lapse camera network, *Hydrology and Earth System Sciences*, 17, 1415–1429, <https://doi.org/10.5194/hess-17-1415-2013>, 2013.

- Goodison, B. E., Ferguson, H. L., and McKay, G. A.: Measurement and data analysis, in: *Handbook of Snow: Principles, Processes, Management and Use*, edited by Gray, D. M. and Male, D. H., pp. 191–274, Pergamon Press, Toronto, Canada, 1981.
- Gruber, S.: Modelling snow water equivalent based on daily snow depths, Master's thesis, University of Innsbruck, 2014.
- 760 Guyennon, N., Valt, M., Salerno, F., Petrangeli, A. B., and Romano, E.: Estimating the snow water equivalent from snow depth measurements in the Italian Alps, *Cold Regions Science and Technology*, 167, <https://doi.org/10.1016/j.coldregions.2019.102859>, 2019.
- Haberkorn, A.: European Snow Booklet – an Inventory of Snow Measurements in Europe, <https://doi.org/10.16904/envidat.59>, 2019.
- Heilig, A., Schneebeli, M., and Eisen, O.: Upward-looking ground-penetrating radar for monitoring snowpack stratigraphy, *Cold Regions Science and Technology*, 59, 152–162, <https://doi.org/10.1016/j.coldregions.2009.07.008>, 2009.
- 765 Helfricht, K., Hartl, L., Koch, R., Marty, C., and Olefs, M.: Obtaining sub-daily new snow density from automated measurements in high mountain regions, *Hydrology and Earth System Sciences*, 22, 2655–2668, <https://doi.org/10.5194/hess-22-2655-2018>, 2018.
- Hill, D. F., Burakowski, E. A., Crumley, R. L., Keon, J., Hu, J. M., Arendt, A. A., Wikstrom Jones, K., and Wolken, G. J.: Converting snow depth to snow water equivalent using climatological variables, *The Cryosphere*, 13, 1767–1784, <https://doi.org/10.5194/tc-13-1767-2019>, 2019.
- 770 International Organization for Standardization: ISO 4355:2013-12-01, 2013.
- Johnson, J. B., Gelvin, A. B., Duvoy, P., Schaefer, G. L., Poole, G., and Horton, G. D.: Performance characteristics of a new electronic snow water equivalent sensor in different climates, *Hydrological Processes*, 29, 1418–1433, <https://doi.org/10.1002/hyp.10211>, 2015.
- Jonas, T., Marty, C., and Magnusson, J.: Estimating the snow water equivalent from snow depth measurements in the Swiss Alps, *Journal of Hydrology*, 378, 161–167, <https://doi.org/10.1016/j.jhydrol.2009.09.021>, 2009.
- 775 Jordan, R.: A One-Dimensional Temperature Model for a Snow Cover: Technical documentation for SN THERM.89, Tech. rep., Corps of Engineers, U.S. Army Cold Regions Research & Engineering Laboratory, 1991.
- Jordan, R., Albert, M., and Brun, E.: Physical Processes within the snow cover and their parametrization, in: *Snow and Climate: Physical Processes, Surface Energy Exchange and Modeling*, pp. 12–69, Cambridge University Press, Cambridge, 2010.
- Keeler, C.: Some Physical Properties of Alpine Snow, Tech. rep., Corps of Engineers, U.S. Army Cold Regions Research & Engineering Laboratory, 1969.
- 780 Kinar, N. J. and Pomeroy, J. W.: Measurement of the physical properties of the snowpack, *Reviews of Geophysics*, 53, 481–544, <https://doi.org/10.1002/2015RG000481>, 2015.
- Koch, F., Henkel, P., Appel, F., Schmid, L., Bach, H., Lamm, M., Prash, M., Schweizer, J., and Mauser, W.: Retrieval of Snow Water Equivalent, Liquid Water Content, and Snow Height of Dry and Wet Snow by Combining GPS Signal Attenuation and Time Delay, *Water Resources Research*, <https://doi.org/10.1029/2018WR024431>, 2019.
- 785 Kojima, K.: Densification of Seasonal Snow Cover, in: *Physics of Snow and Ice : proceedings*, vol. 1 of 2, pp. 929–952, Sapporo, Japan, <http://hdl.handle.net/2115/20351>, 1967.
- Langlois, A., Kohn, J., Royer, A., Cliche, P., Brucker, L., Picard, G., Fily, M., Derksen, C., and Willemet, J. M.: Simulation of Snow Water Equivalent (SWE) Using Thermodynamic Snow Models in Québec, Canada, *Journal of Hydrometeorology*, 10, 1447–1463, <https://doi.org/10.1175/2009JHM1154.1>, 2009.
- 790 Lehning, M., Bartelt, P., Brown, B., Russi, T., Stöckli, U., and Zimmerli, M.: SNOWPACK model calculations for avalanche warning based upon a new network of weather and snow stations, *Cold Regions Science and Technology*, 30, 145–157, [https://doi.org/10.1016/S0165-232X\(99\)00022-1](https://doi.org/10.1016/S0165-232X(99)00022-1), 1999.

- Lehning, M., Bartelt, P., Brown, R., Fierz, C., and Satyawali, P.: A physical SNOWPACK model for the Swiss Avalanche Warning Services. Part II: Snow Microstructure, *Cold Regions Science and Technology*, 35, 147–167, 2002.
- 795 Leppänen, L., Kontu, A., and Pulliainen, J.: Automated Measurements of Snow on the Ground in Sodankylä, *Geophysica*, 53, 45–64, [http://www.geophysica.fi/pdf/geophysica\\_2018\\_53\\_leppanen.pdf](http://www.geophysica.fi/pdf/geophysica_2018_53_leppanen.pdf), 2018.
- López-Moreno, J. I., Leppänen, L., Luks, B., Holko, L., Picard, G., Sanmiguel-Valladolid, A., Alonso-González, E., Finger, D. C., Arslan, A. N., Gillemot, K., Sensoy, A., Sorman, A., Ertaş, M. C., Fassnacht, S. R., Fierz, C., and Marty, C.: Intercomparison of measurements of bulk snow density and water equivalent of snow cover with snow core samplers: Instrumental bias and variability induced by observers, *Hydrological Processes*, 34, 3120–3133, <https://doi.org/10.1002/hyp.13785>, 2020.
- 800 Mair, E., Leitinger, G., Della Chiesa, S., Niedrist, G., Tappeiner, U., and Bertoldi, G.: A simple method to combine snow height and meteorological observations to estimate winter precipitation at sub-daily resolution, *Hydrological Sciences Journal*, 61, 2050–2060, <https://doi.org/10.1080/02626667.2015.1081203>, 2016.
- 805 Marks, D. G., Kimball, J. S., Tingey, D., and Link, T. E.: The Sensitivity of Snowmelt Processes to Climate Conditions and Forest Cover during Rain-on-Snow: A Case Study of the 1996 Pacific Northwest Flood, *Hydrological Processes*, 12, 1569–1587, 1998.
- Martinec, J.: Zimní prognózy s použitím radioisotopu (Winter forecasts with the use of radioisotopes), *Vltavská kaskada (The Vltava reservoir system)*, VUV Praha-Podbab, pp. 45–60, 1956.
- Martinec, J.: Expected snow loads on structures from incomplete hydrological data, *Journal of Glaciology*, 19, 185–195, <https://doi.org/10.3189/S0022143000029270>, 1977.
- 810 Martinec, J. and Rango, A.: Indirect evaluation of snow reserves in mountain basins, in: *Snow, Hydrology and Forests in High Alpine Areas*, 205, pp. 111–120, 1991.
- Marty, C.: GCOS SWE data from 11 stations in Switzerland, <https://doi.org/10.16904/15>, type: dataset, 2017.
- McCreight, J. L. and Small, E. E.: Modeling bulk density and snow water equivalent using daily snow depth observations, *The Cryosphere*, 8, 521–536, <https://doi.org/10.5194/tc-8-521-2014>, 2014.
- 815 Mitterer, C., Hirashima, H., and Schweizer, J.: Wet-snow instabilities: comparison of measured and modelled liquid water content and snow stratigraphy, *Annals of Glaciology*, 52, 201–208, <https://doi.org/10.3189/172756411797252077>, 2011.
- Mizukami, N. and Perica, S.: Spatiotemporal Characteristics of Snowpack Density in the Mountainous Regions of the Western United States, *Journal of Hydrometeorology*, 9, 1416–1426, <https://doi.org/10.1175/2008JHM981.1>, 2008.
- 820 Nash, J. C.: On Best Practice Optimization Methods in R, *Journal of Statistical Software*, 60, 1–14, <http://www.jstatsoft.org/v60/i02/>, 2014.
- Olefs, M., Schöner, W., Suklitsch, M., Wittmann, C., Niedermoser, B., Neururer, A., and Wurzer, A.: SNOWGRID – A New Operational Snow Cover Model in Austria, *International Snow Science Workshop Grenoble – Chamonix Mont-Blanc – October 07-11, 2013*, pp. 38–45, <https://arc.lib.montana.edu/snow-science/item/1785>, 2013.
- Painter, T. H., Berisford, D. F., Boardman, J. W., Bormann, K. J., Deems, J. S., Gehrke, F., Hedrick, A., Joyce, M., Laidlaw, R., Marks, D., Mattmann, C., McGurk, B., Ramirez, P., Richardson, M., Skiles, S. M., Seidel, F. C., and Winstral, A.: The Airborne Snow Observatory: Fusion of scanning lidar, imaging spectrometer, and physically-based modeling for mapping snow water equivalent and snow albedo, *Remote Sensing of Environment*, 184, 139–152, <https://doi.org/10.1016/j.rse.2016.06.018>, 2016.
- 825 Parajka, J., Haas, P., Kirnbauer, R., Jansa, J., and Blöschl, G.: Potential of time-lapse photography of snow for hydrological purposes at the small catchment scale, *Hydrological Processes*, 26, 3327–3337, <https://doi.org/10.1002/hyp.8389>, 2012.
- 830 Paterson, W. S. B.: *The physics of glaciers*, Butterworth/Heinemann, Oxford ; Woburn, MA, 3rd edn., 1998.

- Pistocchi, A.: Simple estimation of snow density in an Alpine region, *Journal of Hydrology: Regional Studies*, 6, 82–89, <https://doi.org/10.1016/j.ejrh.2016.03.004>, 2016.
- Powell, M.: The BOBYQA algorithm for bound constrained optimization without derivatives, Report DAMTP 2009/NA06, University of Cambridge, [https://www.nag.co.uk/IndustryArticles/bound\\_optimization\\_quadratic\\_approximation.pdf](https://www.nag.co.uk/IndustryArticles/bound_optimization_quadratic_approximation.pdf), 2009.
- 835 R Core Team: R: A Language and Environment for Statistical Computing, R Foundation for Statistical Computing, Vienna, Austria, <https://www.R-project.org/>, 2019.
- Rohrer, M. and Braun, L.: Long-Term Records of Snow Cover Water Equivalent in the Swiss Alps, *Nordic Hydrology*, 25, 65–78, <https://doi.org/10.2166/nh.1994.0020>, 1994.
- Sandells, M., Flerchinger, G. N., Gurney, R., and Marks, D. G.: Simulation of snow and soil water content as a basis for satellite retrievals, *Hydrology Research*, 43, 720–735, <https://doi.org/10.2166/nh.2012.028>, 2012.
- 840 Schattan, P., Köhli, M., Schrön, M., Baroni, G., and Oswald, S. E.: Sensing Area-Average Snow Water Equivalent with Cosmic-Ray Neutrons: The Influence of Fractional Snow Cover, *Water Resources Research*, 55, 10 796–10 812, <https://doi.org/10.1029/2019WR025647>, 2019.
- Schellander, H. and Hell, T.: Modeling snow depth extremes in Austria, *Natural Hazards*, 94, 1367–1389, <https://doi.org/10.1007/s11069-018-3481-y>, 2018.
- 845 Seibert, P., Frank, A., and Formayer, H.: Synoptic and regional patterns of heavy precipitation in Austria, *Theoretical and Applied Climatology*, 87, 139–153, <https://doi.org/10.1007/s00704-006-0198-8>, 2007.
- Smith, C. D., Kontu, A., Laffin, R., and Pomeroy, J. W.: An assessment of two automated snow water equivalent instruments during the WMO Solid Precipitation Intercomparison Experiment, *The Cryosphere*, 11, 101–116, <https://doi.org/10.5194/tc-11-101-2017>, 2017.
- Smyth, E. J., Raleigh, M. S., and Small, E. E.: Particle Filter Data Assimilation of Monthly Snow Depth Observations Improves Estimation of Snow Density and SWE, *Water Resources Research*, 55, 1296–1311, <https://doi.org/10.1029/2018WR023400>, 2019.
- 850 Sturm, M. and Holmgren, J.: Differences in compaction behavior of three climate classes of snow, *Annals of Glaciology*, 26, 125–130, 1998.
- Sturm, M., Taras, B., Liston, G. E., Derksen, C., Jonas, T., and Lea, J.: Estimating Snow Water Equivalent Using Snow Depth Data and Climate Classes, *Journal of Hydrometeorology*, 11, 1380–1394, <https://doi.org/10.1175/2010JHM1202.1>, 2010.
- Valt, M., Romano, E., and Guyennon, N.: Snowcover density and snow water equivalent in the Italian Alps, in: *Proceedings ISSW 2018, International Snow Science Workshop*, Innsbruck, Austria, 2018.
- 855 Vionnet, V., Brun, E., Morin, S., Boone, A., Faroux, S., Le Moigne, P., Martin, E., and Willemet, J. M.: The detailed snowpack scheme Crocus and its implementation in SURFEX v7.2, *Geoscientific Model Development*, 5, 773–791, <https://doi.org/10.5194/gmd-5-773-2012>, 2012.
- Wastl, C.: *Klimatologische Analyse von orographisch beeinflussten Niederschlagsstrukturen im Alpenraum*, Phd thesis, Ludwig-Maximilians-Universität München, <http://nbn-resolving.de/urn:nbn:de:bvb:19-95453>, 2008.
- 860 Wever, N., Schmid, L., Heilig, A., Eisen, O., Fierz, C., and Lehning, M.: Verification of the multi-layer SNOWPACK model with different water transport schemes, *The Cryosphere*, 9, 2271–2293, <https://doi.org/10.5194/tc-9-2271-2015>, 2015.

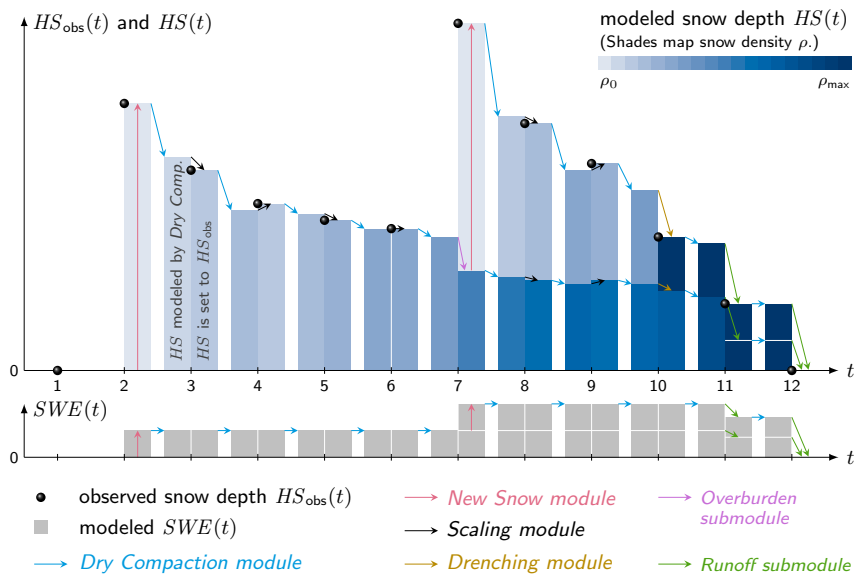


**Figure 1.** Schematic figure of the  $\Delta$ SNOW.MODEL's principles. See text for more details.

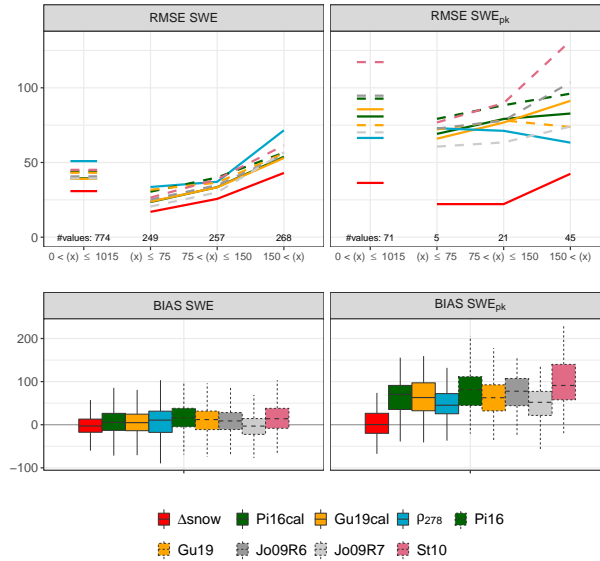


**Figure 2.** Root mean square errors (RMSE) and biases (BIAS) between the  $\Delta$ SNOW.MODEL and different empirical regression models and the  $SWE_{val}$  observations. The  $\Delta$ SNOW.MODEL, Pistocchi (2016)’s and Guyennon et al. (2019)’s models, as well as the “constant density approach” were calibrated with  $SWE_{cal}$  data ( $\Delta$ snow, Pi16cal, Gu19cal,  $\rho_{278}$ ; upper panels, solid lines). Dashed lines indicate the Pistocchi (2016), the Guyennon et al. (2019), the Jonas et al. (2009), and the Sturm et al. (2010) models with their standard parameters (Pi16, Gu19, Jo09R6, Jo09R7, and St10). Jo09R6 and Jo09R7 together illustrate the maximum possible spread of the Jonas et al. (2009) model since Region 6 (R6) and Region 7 (R7) are characterized by the highest and lowest “region-specific offset”, respectively. The upper left panel shows RMSEs for all  $SWE_{val}$  values (short horizontal lines) as well as for three  $SWE$  classes:  $SWE \leq 75$ ,  $SWE > 150$ , and intermediate. Analogously for  $SWE_{pk}$  (upper right panel). The boxes for the biases (lower panels) encompass 774 values (left panel,  $SWE$ ) and 71 values (right panel,  $SWE_{pk}$ ) and spread from the 25%- to the 75%-quantile, the whiskers indicate 1.5 times the interquartile range. Units are  $\text{kg m}^{-2}$ .

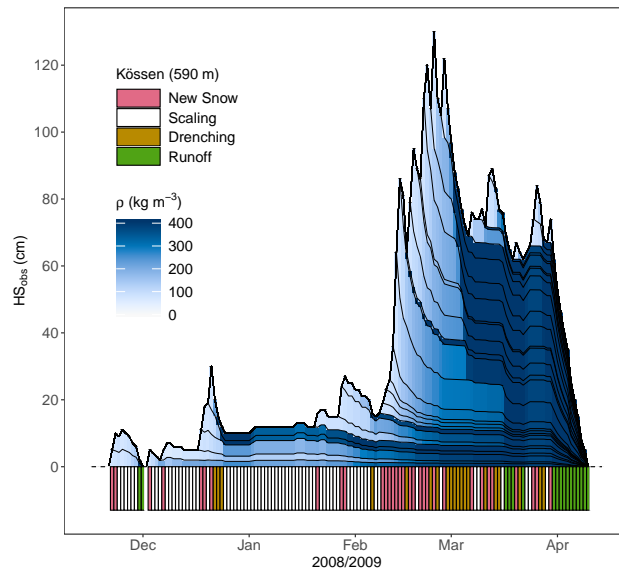


**Figure 3.** Winter of 2008/09 in Kössen (Northern Alps, Austria) portrays density evolution as simulated by the  $\Delta$ SNOW.MODEL. The regular, daily snow depth record is used as only model input. The *New Snow module*, the *Scaling module* and the *Drenching module*, as well as the *Runoff submodule* are depicted in colors at the bottom, whenever activated. Note, the  $\Delta$ SNOW.MODEL is not intended to simulate individual layers, but to calculate daily  $SWE$ ,  $SWE_{pk}$ , and *mean* daily bulk density as accurate as possible. Descriptions and discussions of some features are given in the text.



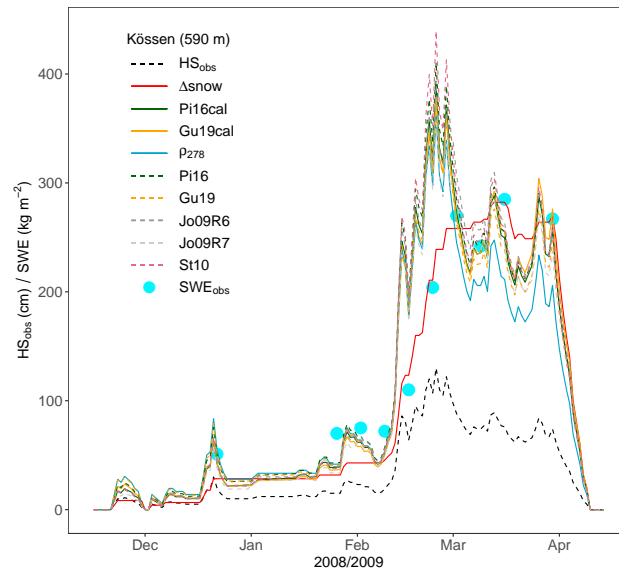


**Figure 4.** *SWE* simulations and observations ( $SWE_{obs}$ ) for the winter 2008/09 in Kössen (cf. Fig. 3). Details and abbreviations are given in the text (Sect. 3.2) and summarized in Fig. 2.

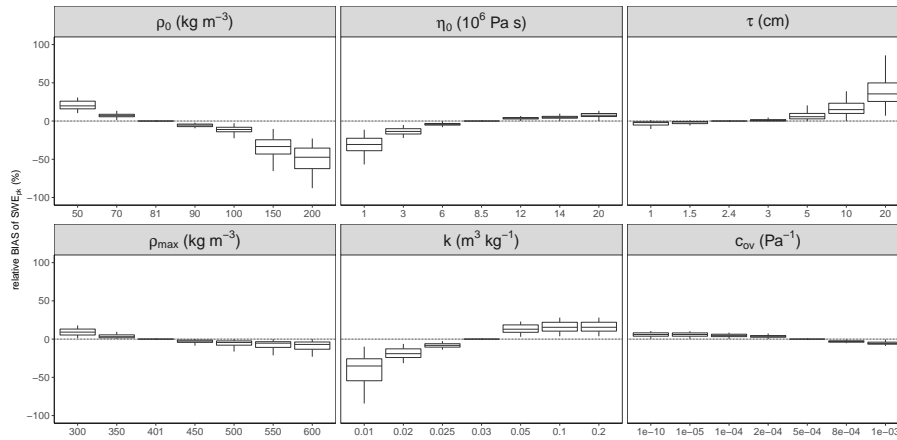


**Figure 5.** Sensitivity of  $SWE_{pk}$  to changes in model parameters. The “relative BIAS of  $SWE_{pk}$ ” is defined as the difference between  $SWE_{pk}$  with best-fitted values and  $SWE_{pk}$  with changed parameters (while all others are kept unchanged), divided by the best-fitted  $SWE_{pk}$ . The boxes comprise  $SWE_{pk}$  of all stations and all years of the validation data set  $SWE_{val}$  (71 values) and display medians as well as 25% and 75% percentiles, the whiskers indicate 1.5 times the interquartile range. Details and analysis see text.

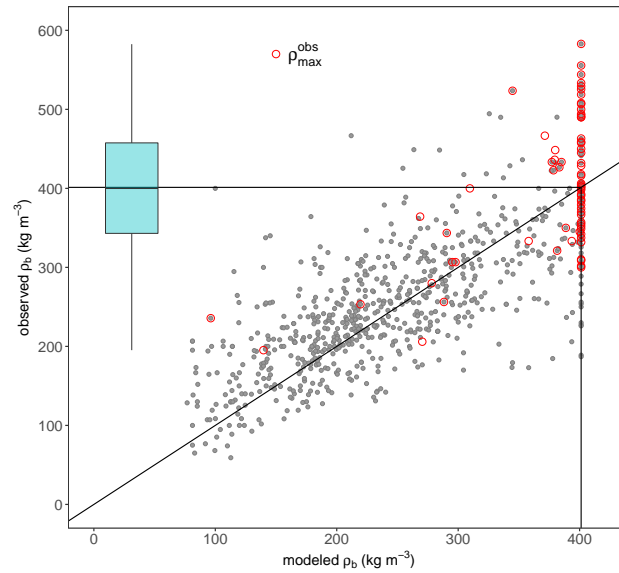


**Figure 6.** Scatter plot of all modeled bulk snow densities  $\rho_b$  versus all observed  $\rho_b$  from the validation data set. ( $SWE_{\text{val}}$ , 767 data pairs. Seven observations, which are higher than  $600 \text{ kg m}^{-3}$ , were ignored due to implausibility.) Red circles reflect the 71 observed yearly maxima ( $\rho_{\max}^{\text{obs}}$ ), most of them occur when also modeled snowpack is at  $\rho_{\max} = 401 \text{ kg m}^{-3}$ . The box plot shows the distribution of  $\rho_{\max}^{\text{obs}}$  with median, 25% and 75% percentiles, and whiskers at 1.5 times the interquartile range.

**Table 1.** Different types of *SWE* models, categorized by their essential input. TD, SE, and ERMs are abbreviations for thermodynamic, semi-empirical, and empirical regression models, respectively.

essential input	TD	SE	ERMs
<i>HS</i> (single values)			x
<i>HS</i> (regular records)	x <sup>a</sup>	x	
one or more atmospheric variable(s)	x		
date	(x) <sup>b</sup>		x
location parameters <sup>c</sup>	(x) <sup>b</sup>		x

<sup>a</sup>or another precipitation input

<sup>b</sup>only essential in some cases, e.g. for parameterizations

<sup>c</sup>altitude, regional climate, etc.

**Table 2.** Summary of compaction processes and processes forcing mass changes that are integrated in the modules and submodules of the  $\Delta$ SNOW.MODEL, and of processes that are ignored.

<i>module</i>	process
<i>New Snow</i>	significant rise of <i>HS</i> , enhanced compaction due to overburden load ( <i>Overburden submodule</i> )
<i>Dry Compaction</i>	significant decline of <i>HS</i> due to dry metamorphism <sup>a</sup> and/or deformation <sup>a</sup>
<i>Drenching</i>	significant decline of <i>HS</i> due to wet metamorphism <sup>a</sup> , runoff through melt ( <i>Runoff submodule</i> )
<i>Scaling</i>	adjustments to small changes of <i>HS</i> within threshold deviation $\tau$
ignored:	snow drift compaction <sup>a</sup> and mass changes due to: rain-on-snow, runoff during snowfalls, wind drift, small snowfalls, sublimation and deposition

<sup>a</sup>terminology follows Jordan et al. (2010)

**Table 3.** The seven parameters of the  $\Delta$ SNOW.MODEL. The last column depicts model sensitivity to changes in the density parameters. The respective gradients are means over the whole calibration ranges.

Parameter <i>par</i>	unit	optimal value	calibration range	literature range	sensitivity $\frac{\delta SWE_{pk} [\text{kg m}^{-2}]}{\delta par}$
$\rho_0$	$\text{kg m}^{-3}$	<b>81</b>	50-200	75 <sup>a</sup> , 10-350 (70-110) <sup>b</sup>	+0.37 (+0.50 <sup>†</sup> )
$\rho_{\max}$	$\text{kg m}^{-3}$	<b>401</b>	300-600	450 <sup>c</sup> , 217-598 <sup>d</sup> , 400-800 <sup>e</sup>	+0.24
$\eta_0$	$10^6 \text{ Pa s}$	<b>8.5</b>	1-20	8.5 <sup>a</sup> , 6 <sup>f</sup> , 7.62237 <sup>g</sup>	not calc.
$k$	$\text{m}^3 \text{ kg}^{-1}$	<b>0.030</b>	0.01-0.2	0.011-0.08 <sup>a</sup> , 0.185 <sup>b</sup> , 0.023 <sup>f,g</sup> , 0.021 <sup>i</sup>	not calc.
$\tau$	cm	<b>2.4</b>	1-20	-	not calc.
$c_{\text{ov}}$	$10^{-4} \text{ Pa}^{-1}$	<b>5.1</b>	0-10	-	not calc.
$k_{\text{ov}}$	-	<b>0.38</b>	0.01-10	-	not calc.

<sup>a</sup>Sturm and Holmgren (1998), <sup>b</sup>Helfricht et al. (2018) with range for means in brackets, <sup>c</sup>Rohrer and Braun (1994), <sup>d</sup>Sturm et al. (2010), <sup>e</sup>Paterson (1998), <sup>f</sup>Jordan et al. (2010), <sup>g</sup>Vionnet et al. (2012), <sup>h</sup>Keeler (1969), <sup>i</sup>Jordan (1991). See Sect. 2.3 for more details. <sup>†</sup>The value in brackets is the gradient taken from the smaller window between 70 and 90  $\text{kg m}^{-3}$  (cf. Sect. 4.1).

**Table 4.** Overview on  $SWE$  accuracies of different models and studies. The numbers in brackets represent the results for the example portrayed in Figs. 3 and 4 from station Kössen in 2008/09. Units are  $\text{kg m}^{-2}$ , TD is short for thermodynamic snow models. Model abbreviations see caption of Fig. 2.

source	model (version)	$SWE$ BIAS	$SWE$ RMSE	$SWE$ MAE	$SWE_{\text{pk}}$ BIAS	$SWE_{\text{pk}}$ RMSE
this study	$\Delta$ SNOW.MODEL	-3.0	30.8 (21)	21.9	0.3 (-3)	36.3
	Gu19cal	4.8	39.1 (43)	27.6	63.0 (93)	85.6
	Pi16cal	5.6	39.4 (47)	28.1	70.3 (106)	80.8
	Jo09R7	-3.2	39.4 (41)	27.3	52.0 (74)	70.2
	St10	14.0	45.1 (57)	32.6	91.1 (154)	117.2
	$\rho_{278}$	10.6	50.9 (51)	36.3	45.2 (77)	66.4
Guyennon et al. (2019)	Gu19			49.2		
	Pi16cal			50.6		
	Jo09cal			48.5		
	St10cal			51.0		
Jonas et al. (2009)	Jo09		50.9 – 53.2			
Sturm et al. (2010)	St10 (“alpine”)	29 ± 57				
Vionnet et al. (2012)	Crocus	-17.3	39.7			
Langlois et al. (2009)	Crocus	-7.9 to -5.4	10.8 – 12.5			
	SNTHERM	9 to 18.1	18.3 – 19.3			
	SNOWPACK	-0.1 to 5.6	7.4 – 14.5			
Egli et al. (2009)	SNOWPACK		56			
Wever et al. (2015)	SNOWPACK		ca. 39.5			
Sandells et al. (2012)	SNOBAL		30 – 49			17 – 44 <sup>a</sup>
Essery et al. (2013)	various TD <sup>b</sup>		23 – 77			

<sup>a</sup>This is not RMSE of  $SWE_{\text{pk}}$ , but RMSE “from establishment of snowpack to  $SWE_{\text{pk}}$ ”. <sup>b</sup>See Essery et al. (2013)’s Table 10: RMSE for up to 1700 uncalibrated and calibrated simulations.

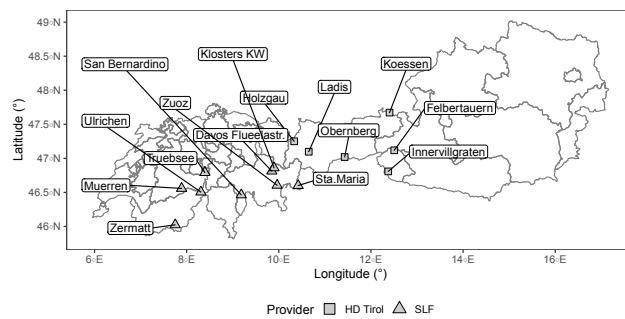


**Figure A1.** Locations of the stations used for calibration and validation. Austrian stations are operated by the Hydrographic Service of Tyrol (HD Tirol), the Swiss stations by the WSL Institute for Snow and Avalanche Research SLF. See Table A1 and text for more details.



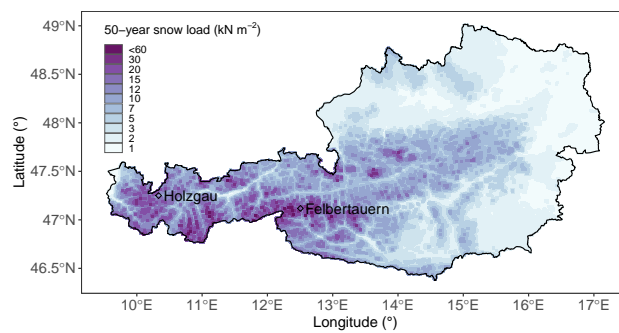


**Figure A2.** 50-year return levels of snow load in Austria. Two stations with *SWE* observations are outlined for a qualitative validation. This map bases on 214 snow depth records,  $\Delta\text{SNOW.MODEL}$  derived *SWE*, and smooth spatial modeling of their extremes.

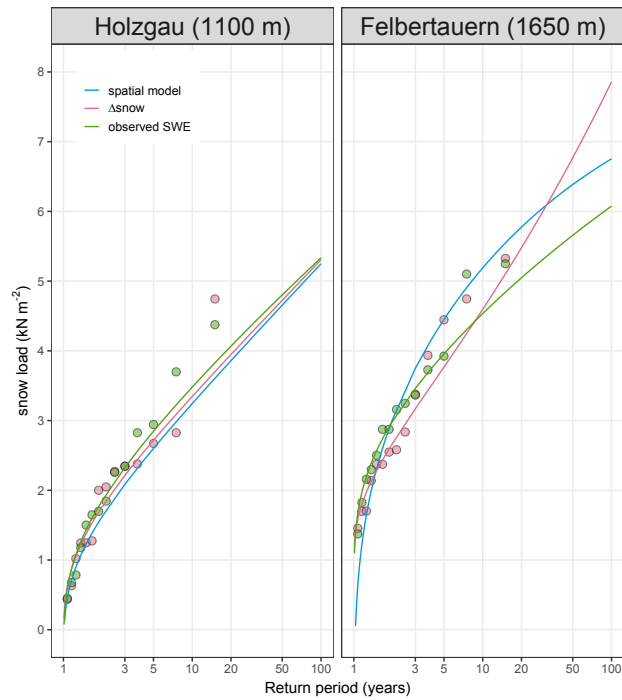


**Figure A3.** Return levels of snow load at stations Holzgau (left) and Felbertauern. Return periods in years are shown on the logarithmic x-axis. The blue line shows return levels obtained with the spatial extreme value model, pink bullets and lines depict yearly maxima and the GEV fit of *SWE* values modeled from daily snow depths with the  $\Delta$ SNOW.MODEL, and green colors represent yearly *SWE* maxima and the corresponding GEV fit from (ca. weekly) observations.

**Table A1.** Overview of stations with daily snow depths record and about weekly/biweekly (Austria/Switzerland) manual *SWE* observations which were used for calibration and validation.  $\#_{\text{cal}}^{\text{SWE}}$  and  $\#_{\text{val}}^{\text{SWE}}$  give the numbers of respective manual *SWE* observations. Stations #1 to #6 are located in the Austrian province of Tyrol, #5 and #6 are in the sub-province of Eastern Tyrol; all operated by the Hydrographic Service of Tyrol. Swiss stations #7 to #15 are operated by the WSL Institute for Snow and Avalanche Research SLF. Compare Fig. A1. The data sources are Gruber (2014) and Marty (2017).

#	station name	lon [°]	lat [°]	alt [m]	$\#_{\text{cal}}^{\text{SWE}}$	$\#_{\text{val}}^{\text{SWE}}$	calibration seasons <sup>a</sup>	validation seasons <sup>a</sup>
1	Holzgau	10.333300	47.25000	1100	116	100	7 odd in 1999-2011	7 even in 1998-2010
2	Ladis	10.649200	47.09690	1350	83	66	7 odd in 1999-2011	6 even in 1998-2010 <sup>b</sup>
3	Obernberg	11.429200	47.01940	1360	105	88	7 odd in 1999-2011	7 even in 1998-2010
4	Koessen	12.402800	47.67170	590	87	70	7 odd in 1999-2011	6 even in 1998-2010 <sup>b</sup>
5	Felbertauern	12.505600	47.11810	1650	126	114	7 odd in 1999-2011	7 even in 1998-2010
6	Innervillgraten	12.375000	46.80830	1400	96	115	7 odd in 1999-2011	7 even in 1998-2010
7	Muerren	7.890193	46.55818	1650	37	27	2009,2012,2015,2017	2006,2011,2014,2016
8	Truebsee	8.395291	46.79121	1780	4	11	2016	2015,2017
9	Ulrichen	8.308283	46.50461	1350	24	23	2009,2013,2015,2017	2007,2011,2014,2016
10	Zermatt	7.751165	46.02340	1600	47	76	1961,1963 and 7 even in 2004-2016	3 even 1960-1964, 7 odd in 2005-2017
11	Davos Flueelastr.	9.848163	46.81255	1560	8	19	2012	2008,2017
12	Klosters KW	9.895973	46.86058	1200	12	22	1999	1998,2017
13	San Bernardino	9.184634	46.46326	1640	11	14	2007	2006,2014
14	Sta.Maria	10.419344	46.59981	1415	0	8	-	1969
15	Zuoz	9.962676	46.60433	1710	24	21	2011,2013,2015,2017	2006,2012,2014,2016
$\Sigma$					780	774	67	71

<sup>a</sup>Indicated years mark the start of respective winter seasons. <sup>b</sup>2006 is missing.